

The Rubberized Mechanical Features: Hardness, Modulus, Tensile Strength, Elongation at Break and Aging for Manufacturing Automotive Tires-An Overview

Md. Ekhlass Uddin ^{1,2}, Md. Faruk Hossen ³, Md. Ali Asraf ⁴, Md Rausan Zamir ⁵
and Md. Kudrat-E-Zahan ^{6*}

^{1,2} Department of Chemistry, Rajshahi University and Chemist, Apex Husain Ltd, Bangladesh

³ Department of Chemistry, Rajshahi University, Bangladesh

⁴ Department of Chemistry, Rajshahi University, Bangladesh

⁵ Department of Chemistry, Rajshahi University, Bangladesh

⁶ Department of Chemistry, Rajshahi University, Bangladesh

Abstract: Both rubber physics and chemistry are utilized for the manufacturing of spacecraft treads, tires, vehicle mats, conveyor belts, etc., in industries related to the automobile. This versatile rubber technology is devoted to vast and excellent mechanical features like hardness, modulus, tensile strength, elongation at break, and thermal aging. The science and practice of rubber compounding during the processing of tires provided rheological, mechanical properties, and stress-strain properties with aging are discussed in this technical review. Differential Scanning Calorimetry (DSC) reveals intricate phase transitions of microstructural changes. Thermogravimetric Analysis (TGA) offers information on the thermal stability of chemical compositions and the glass transition point, establishing operational flexibility for rubber characteristics in this investigation. However, these combined resources will thoroughly grasp the material's features, facilitating improved tire product design and quality assurance.

Keywords: Natural rubber, Synthetic rubber, Mechanical hardness, Modulus, Tensile strength, Elongation at break, Thermal aging, Tire industry.

1. Introduction

Natural rubber as a polymer is an inexhaustible material widely utilized in various industries, mainly for automotive, aerospace, food, pharmaceutical tires, and more than ¹⁻³. The automotive industry is the largest user of rubber products, following its mechanical properties: resistance to oil, heat, hydrocarbons, solvents, flame retardant, impermeability to gases and volatile substances, and resistance to water and steam since natural rubber is a natural elastomer that has superior features, particularly elasticity, and has the power to generate its original state when stretched with a load ⁴⁻⁷.

Test samples applied for mechanical props were cut from the dumbbell specimen ⁸. The thermoplastic dynamic of fresh rubber compositions is vulcanized with the best mechanical performance possessed by natural rubber (NR), styrene-butadiene rubber (SBR), and ethylene propylene diene rubbers (EPDM) rubbers with ground tire rubber (GTR). The type of accelerator is widely employed for NR, SBR, EPDM, etc. (Fig. 1), relying on the significant ingredients that

decide the mechanical distribution of the filler in the rubber and the vulcanizing structure according to DSC and TGA analysis ⁹. Chemical exchange of some operative groups of rubbers also happens throughout their mastication or age ¹⁰. Vulcanization (curing, cross-linking) is one of the essential and well-known processes for most of the rubber technologies ¹¹. The rubber industry commenced developing the use of sulfur in natural rubber. The addition of sulfur in a natural rubber matrix is carried out to improve the vulcanization processes that form cross-linking by producing better mechanical properties ¹². Moreover, vulcanizing with polysulfide cross-links possesses a higher tensile value than vulcanizing with monosulfide and carbon-carbon cross-links. Elongation at break is when the increasing crosslink density is lowered at first. Then, it is asymptotically neared to the minimum value where the highest structural strength has soft under-vulcanized features under optimum glass transition points ¹³⁻¹⁵. Reclaimed rubber is one of the options for minimizing the environmental pollution that comes from extravagant consumption of rubber products, especially tire production ¹⁶⁻¹⁹. The increased reclaimed rubber ratio

*Corresponding author: Md. Kudrat-E-Zahan

Email address: kudrat.chem@ru.ac.bd

DOI: <http://dx.doi.org/10.13171/mjc02501061807Zahan>

Received September 4, 2024

Accepted January 2, 2025

Published January 6, 2025

efforts decrease tensile, tear strength, and elongation at break (%) but increase the tensile modulus by 100% (M100) ²⁰⁻²⁵. SBS/CRP-reinforced bitumen is urged for implementation in plateau fields compared to original bitumen and SBS-modified bitumen. Naturally, it is hinted that the low-temperature advancement of SBS/CRP-functionalized bitumen under different temperatures can analyzed in future research ²⁶⁻²⁷. End-of-life tires and their degradation present severe environmental concerns owing to their resistance to oxygen, ozone, UV light, heat, etc.

Research has been put forward that the addition of rubber waste has enhanced the mechanical attributes of the blends, such as bettered tensile strength and modified impact strength, and has eminent potential in many applications ²⁸⁻³¹.

However, the overview rivets on the optimum conditions: hardness, modulus, tensile strength, elongation at break, and aging for making solid tires have been established by DSC and TGA analysis.

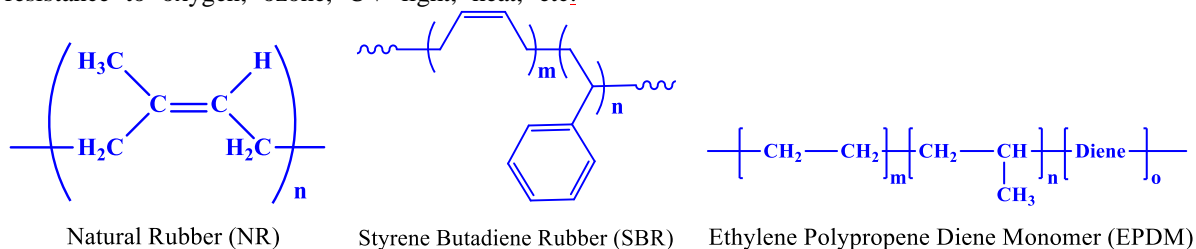


Fig. 1. The chemical structures of some highly used natural rubber and synthetic rubber in rubber industries

2. Mechanical Features

2.1. Hardness

Susanto et al. studied how hardness increased with the longer length age using a Shore-A hardness tester for tire manufacturing ³². They ornamented the plot for hardness (Shore-A) against Resorcinol Formaldehyde (DRF) concerning the variant aging hour (0, 12, 24, 48, and 72 hours). Based on the curing characteristics, it was exhibited that DRF content was used as a fresh filler in natural rubber-styrene butadiene rubber composites due to its ability to improve hardness with an oven duration of 72 hours. The effect of thermal steps and starch loading on the hardness of

SBR/NR/DRF composites performed at the hardness level 50-55 (Shore-A) with DRF content (25 phr). *Muller et al.* exhibited that the hardness decreased with the gradual addition of active rubber powder (ARP) to the adhesive bond strength of two-component epoxy resin ³³. Composite material ARP5 to ARP30 matrix visualized the hardness between the laboratory environment and the cyclic degradation at the significance level of 0.05. By adding ARP into the matrix, the hardness potentially dropped up to 71% among the tested polymers assessed by the physical notification of a solid tire (Fig. 2).

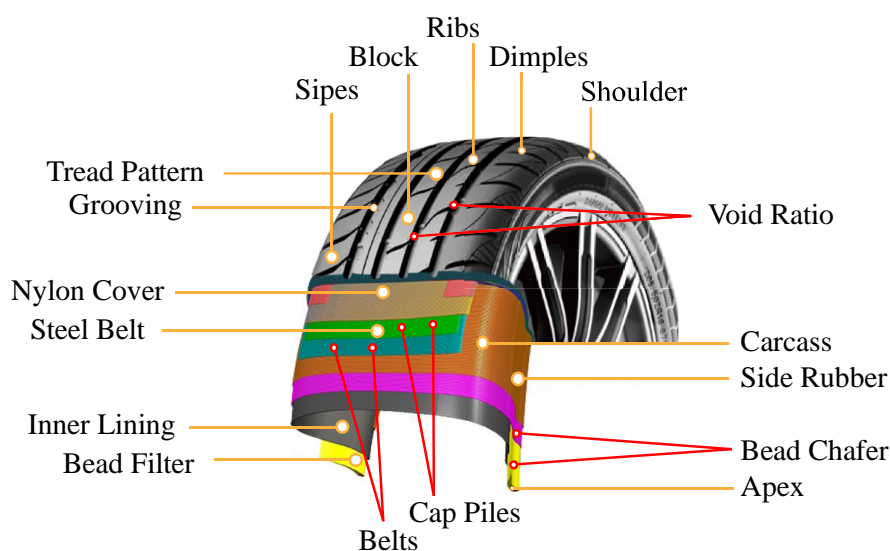


Fig. 2. The physical notification of a solid tire

Dan et al. used mechanical hardness to mix the coconut coir fiber with the waste tires by durometer ³⁴. The largest hardness (21.04) was observed when 80% waste rubber (WR) was engrafted with 10% coir fiber (CF) and 10% polypropylene (PP) 10 times

rather than the mixture 85% WR + 5% CF + 10% PP. Furthermore, the gasket possessed more resistivity to evaluate hardness to prevent leakage compressed by the pipe, as the higher the hardness, the higher the localized deformation of the compounds. The liquid

contaminants: diesel oil, NPK fertilizer, sodium chloride solution, and rainwater tempted the hardness value of agricultural tire tread in the degradation medium assessed by Muller et al.³⁵. Diesel oil played a vast role in increasing tire hardness compared to NPK fertilizer, solutions of water, NaCl, and rainwater on the tire rubber. The appreciable Shore-A hardness at series 1 possessed 8% on average. At series 2, it was 37% on average for the diesel oil-impacted tire, which decreased and occurred at tire 2A, compared to the significant hardness of 2C and 2B at a consuming time 2 h. The arithmetical mean data found in intervals 0, 1, 2, 3, 4, 6, 10, and 16 weeks and 1C specimen in water/NPK medium accurately exposed the hardness of 73.63 Shore-A. L-cystine (L-cys) and its derivative L-cystine-dimethyl ester dihydrochloride (ELCH) displayed the potential hardness and be used as a worthy substitute of N-N-Di-phenyl Guanidine (DPG) for the formulation of silica-filled styrene butadiene-rubber (S-SBR) tires by Debnath et al.³⁶. The silica-filled waste products showed the highest hardness of 73.9 Shore-A, whose values in the parenthesis dictated the percentage increase. Lee et al. described the hardness level of poly-ketone fiber-modified natural rubber composites at different temperatures (105°C, 125°C, and 180°C)³⁷. It was quite obvious that the hardness increased due to oxidation or crumbling of the surface cross-linking at 125 °C. The remarkable degradation occurred at 180 °C, followed by thermal aging, which determined the increasing hardness rate for poly-ketone/NR composites. The hardness of the composite during thermo-oxidation at 180°C was found to be, on average 80-85. Wright et al. found that meaningful rubber hardness was measured roughly 15 times with 10 locations on the tread and sidewall to modify the tire model³⁸. Although the tread hardness pushed aside the noteworthy level, the sidewall showed an effective hardness alteration after the first aging cycle. However, the percentile change in Shore-A hardness at the tread was 6% compared to the sidewall of >10%. Hardness was potentially raised with increasing marble sludge (MS) content in the rubber compound described by Ahmed et al.³⁹. The hardness values were performed with the trend of parts per hundred rubber (pphr): MS: 00< 10< 30< 50< 70< 90, where the MS-filled NR composites were higher compared to that of the unfilled NR compound (MS 00: original value = 36; Aging at 70°C for 96 h = 39; Aging at 100°C for 96 h = 40). This is how the hardness of NR composites was enhanced with the increase in stiff marble sludge content (µm). The filler feature of carbon black (CB) was functionalized with sulfur in thioglycolic acid. It produced a very effective cross-linked polymer meshwork, which accelerated the vulcanization and produced the authentic hardness screened out by He et al.⁴⁰. Bandyopadhyay et al. investigated the tenuous decrease in hardness of regenerated black compounds⁴¹. These compounds were characteristically defined during the comparison with a virgin N330 black executed from waste automobile tire tread. Consequently, all compounds

performed the largest hardness value, which provided approximately an equivalent range due to the slight breakage and aberration of the heat-interposed regenerated black on a bias tire tread cap compound. Here, the 0% regenerated black provided higher hardness than <100% regenerated black with Silicon-69. The hardness of rubber of a simple tire-specific model was evaluated based on oven measuring noise levels between Standard Reference Tire Type (SRTT) and Avon AV4 tires (0.05 units and 0.1 units Shore-A, respectively) by Buhlmann et al.⁴². They developed the tire rubber hardness of in-service CPX reference tire sets and plotted the number of measurement days (season 2012: March to October) against tire rubber hardness [unit Shore-A]. The effective linear relationship of rubber hardness was found to be raised by 3.1 units Shore-A for the SRTT tires and by 6.3 units Shore-A for the Avon AV4 tires. Additionally, SRTT and Avon AV4 tires released tire/road noise levels with a proliferative rate of +0.3 dB (A) and +0.15 dB (A) per unit Shore-A, respectively, referring to Dense Asphalt Concrete (DAC) 0/16 road surface. However, Avon AV4 exhibited the highest hardness at 70.1 Shore-A compared to SRTT. The filler functionalization of SBR was another important recognition to develop the hardness of the pyrolysis carbon black likened to virgin pyrolysis carbon black of waste tires by Delchev et al.⁴³. The hardness values of the pyrolysis carbon black reinforced rubber compounds were in the following ascending order: SBR 1 <SBR 3 <SBR 2 <SBR 4. The hardness value of the vulcanized ground tire rubber (D-GTR) was observed with and without the addition of carbon black, respectively. Consequently, the hardness was found to be less without the addition of D-GTR. The experiment exhibited that the adjustment of carbon black at 50 phr D-GTR content provided the highest hardness concerning virgin tire tread and other modified D-GTR content (10 and 30 phr). Moreover, D-GTR functionalized carbon black enhanced the hardness values owing to the lower elastomer in the matrix based on the properties of a passenger car tire tread formulation⁴⁴. Lignin functionalized elastomer, butyric, and isobutyric lignin slightly enhanced the stiffness than carbon black for the development of sustainable tire technology monitored by Ismail et al.⁴⁵. For waste rubber recycling, high-density polyethylene (HDPE): H-R10-P compounds had higher hardness values except for H-R10 and H-R10-C. However, the hardness of both NR and NBR compounds was increased up to 98 Shore-A for LDPE/NBR (80/20) blends functionalized with MA-grafted particles⁴⁶. Pal et al. tested the hardness of 'NSU-5' and 'NSU-6' rubber specimens and found that the hardness was higher than the blends by the squeeze of Intermediate Super Abrasion Furnace (ISAF) carbon black⁴⁷. The strong cross-link density increases the hardness of those rubber compounds. Ramarad et al. also determined the hardness by raising the ground tire rubber/reclaimed tire rubber (GTR/RTR) loading owing to the larger crosslink

showed the best stiffness, affecting the creep recovery behavior. The complex moduli were plotted against the reduced frequency (rad/s) and the decrement with the oxidative system, in which both G^* and δ values were qualified for the conventional and activated samples. It is seen that the storage modulus was opposite to the stiffness ratio as the loading frequency was increased at 60 °C. The moduli were directly prepared for the antiphony substitution of Crumb Rubber (CB) by multi-walled carbon nanotubes (MWCNTs) with the same weight percentage. In this case, *Poikelispaa et al.* narrated the total volume fraction of the makeweights for higher MWCNT diluting⁵¹. The 100% modulus departs to raise after internalization of 2 phr MWCNTs, and an intimately twofold step-up in 100% modulus is bumped at 12.5 phr MWCNTs, assuring the composite carrying only CB. When the compound is filled only with CB and, as much as possible, the MWCNTs are comfortably spread out. The polymeric interaction occurs so that the largest surface area of the MWCNTs raises the 100% modulus. On the other hand, the measured modulus was required as log strain (%) for MWCNT 12.5 represented as the storage modulus of MWCNT/CB filled NR/BR matrix at 0.56% strain with various concentrations of MWCNTs at 100°C. The highest storage modulus at low strain was 2.56 ± 0.12 for 12.5/12.5 MWCNTS/CB, exhibiting a powerful network shaped by the MWCNTs as CB is, in turn, substituted⁵². 12% waste tire rubber (WTR) + 4% amorphous poly alpha olefin (APAO) and 15% WTR + 4WTR + 4% APAO reinforced asphalt mixture (AC-13C type) illustrated an optimum higher modulus value, which was performed by *Yan et al.*⁵³. The resilient modulus trial at 25°C exhibited that the modulus of the 12% WTR + 4% APAO functionalized asphalt mixture raised most importantly, which was near to twice the modulus of matrix asphalt admixture. The modulus of 15% WTR+415% WTR+4% APAO modified asphalt admixture was also to a greater extent than doubling that of ground substance asphalt. However, the indirect tensile resilient modulus of the asphalt mixture was tested at 25 °C, and the asphalt mixture, type 12W + 4A, exhibited the highest modulus above 6000 MPa. *Carvalho et al.* analyzed the rate of 100% modulus (M_{100}) change in field tires⁵⁴. The crosslink density increases M_{100} to an aerobic condition and at lower temperatures. It was visualized that when the temperature was raised above 80°C, and thermo-oxidative steps possessed aerobic at higher temperatures, M_{100} and consequently a maximum level was found to be for crosslink density. Since the change in M_{100} is concerned with the change in crosslink density for aerobics at lower temperatures, compound A showed the highest modulus of >9 MPa at 60 °C for the square root of aging time, $t^{1/2}$. The bromobutyl content, carbon black with oil levels, etc., potentially contributed to the reasonable modulus provided the optimum impermeability⁵⁵. *Ali et al.* developed the crumb rubber content of rubberized bitumen binder, providing the modulus effects:

complex shear modulus (G^*), storage modulus (G'), and loss modulus (G'')⁵⁶. Here, the viscoelastic features of rubberized bitumen screening and an increase in storage modulus were especially significant, with fewer increases in loss modulus. The modulus ratio increased storage modulus compared with those in loss modulus, preferring the oxidative degradation of rubber. The results showed that the G^* of bitumen binder bearing different substances of crumb rubber was raised after two different thermo-oxidations., the slope of the G^* decreased with increased crumb rubber tightness, implying that crumb rubber built the bitumen binder. CR 16% performed the highest G' of >1200 Pa than CR 0% and CR 8%, where the peak value of G'' was 1200 Pa for CR 16%. *Hassan et al.* put out the resilient modulus study, which was typically used to measure mixtures' ability to retract upon bringing out the applied stresses⁵⁷. The retrievable deformation can appraise resilient modulus to the corresponding resilient strain. The modulus of rubber-reinforced mixtures was to generically increase with increasing rubber capacity, marching the increased elasticity of the mixtures. The crumb rubber capacity of G^* increased in the range of 8–16% and performed an increase of about 1.5–2 times for mature binder than unripe binder by *Ali et al.*⁵⁸. The result demonstrated that G^* depicted the largest value in the 3000-3500 MPa range against crumb rubber content (16%). Since the rubber capacity was raised at 8–16%, the modulus ratio showed a spectacular decrease for aged binder than immature binder. The modulus was especially potentially characterized by the dynamic stiffness of unmodified and modified asphalt concrete mixtures under a longer loading time. However, the modified asphalt mixtures with 10% crumb rubber exhibited an ameliorated modulus equated to the unadjusted asphalt concrete intermixture⁵⁹. *Jaafar et al.* found the significant efficacy of modulus by using liquid natural rubber (LNR) for automotive practical applications⁶⁰. Here, 3 phr of liquid rubber MG30 is tested with epoxy/silica/kenaf composite and demonstrated the highest value (3.51 GPa) for modulus to increase the substantial mechanical property. *Hassan et al.* monitored the resilient modulus of the samples, which decreased regardless of rubber size and content when the temperature dramatically increased. Again, adding a larger amount of crumb rubber decreased the mixtures' resilient modulus. At 25°C, the mixture with fine crumb rubber executes better than the mixture with coarse crumb rubber and with fine and coarse crumb rubber compounding, irrespective of the amount of crumb rubber. At 40°C, the conflict in the resilient modulus between the rubberized and control asphalt mixtures was very tenuous. The resilient modulus for all rubberized asphalt mixtures with 1.5% crumb rubber corresponded to the assessment for the control sample. Nonetheless, the specimen carrying crumb rubber was designated a marginally resilient modulus, which equated to that of the control mixture, excluding sampling with fine crumb rubber. The

resilient modulus of conventional rubber content (0%) provided the highest value of 2314 MPa, higher than coarse crumb rubber at 25°C, where all contents were found in the range of 300–400 MPa at 40°C^{61, 62}. Zedler et al. visualized the short-term devulcanization of ground tire rubber in which the samples with higher bitumen substance preferred higher stiffness to microwave treatment⁶³. It was clear that the specimen GTR+0.5B-MW performed the highest modulus of $M_{100}=4.7$ MPa based on the negligible impact of bitumen plasticizer on reclaimed GTR. Loderer et al. observed that adding CR to bitumen gains the complex modulus at high temperatures and reduces stiffness at low temperatures⁶⁴. The complex modulus of CR-modified bitumen (CRMB) was significantly higher at high temperatures in the styrene-butadiene-styrene (SBS) curve was dislodged sparingly upwards, pointing a larger modulus over the total temperature level. All CRMBs displayed a little more temperature susceptibleness than neat, and the leveling of the complex modulus curve signaled SBS. It was reasoned that adding CR to bitumen increases the stiffness at high temperatures and dampens the ring binder at low temperatures. The given procedure evaluated the fluctuation of G' and G'' at 0.1 Hz for 5°C–45°C, noting that temperature has a significant potentiality on both storage and loss modulus. It was clear that G'' is higher than G' for all binders, showing that the viscous part of the complex modulus is prevalent. The difference between G' and G'' studied the largest for the neat bitumen, particularly at higher temperatures, and the significant effect on the complex modulus's interaction between elastic and viscous factors. Obviously, the modulus 100 (M_{100}) values of all SBR-based vulcanized fibers increase at higher filler quantities. The increment of M_{100} values of vulcanization containing less filler was lower (11%) in case of alteration, while that of vulcanization containing higher filler quantity was more pronounced (17.5%). Modulus 300 (M_{300}) was achieved for virgin pyrolysis carbon black equal to 50 phr carbon black, where the value of M_{100} for vulcanizing qualified pyrolysis carbon black increases partially when compared to vulcanization containing virgin pyrolysis carbon black^{65–70}. On the other hand, Habibah et al. assessed the modulus (M_{100} and M_{300}) of the entities containing various amounts of D-GTR with and without carbon black modification, respectively⁷¹. It might be concluded that adding D-GTR without further addition runs to minify the modulus at 100% and 300% elongation. The internalization of extra carbon black heightens the modulus values owing to the brown elastomer in the matrix. M_{100} was the highest for both 30 phr and 50 phr D-GTR contents (>2 MPa) without adjustment of carbon black than the virgin tire tread, where the M_{100} value was the largest for only 10 phr D-GTR content (>8 MPa). Russell et al. studied the impact of variable concentrations of crumb rubber on the Trinidad Lake Asphalt (TLA)⁷². The complex modulus (G^*) fluctuated at different frequencies and a constant

temperature of 80 °C for the different mixtures. It was also indicated that the G^* was raised with crumb rubber for the material's stiffness. About 5% of the asphalt rubber mixture acquired a modulus 25 times more than the unmodified TLA at 15.9 Hz. In contrast, the complex modulus for the equal blend was roughly 95 times that of the unmodified TLA at 0.1 Hz. Dias et al. displayed the lowest stiffness modulus of TB3 (mixed above 190°C) with that of the reference mixture, TB0 produced without crumb rubber increased with the frequency⁷³. Moreover, the stiffness values of TB0 were measured at 30 and 40 °C, achieving the stiffness observed at 20 °C for the mixture without rubber. In the meantime, AR dry TB3, in which the binder held appreciable stiffness rates, was reduced to 63% and 53% for the equivalent temperature conditions. The reduction of stiffness moduli was obtained for the frequency of 10 Hz, which was used to represent the upshot of high temperature on the modulus of the blends, where TB0 suffered a reduction of 63 MPa at 20–30 °C. Again, the AR dry TB3 and TA determined a partially higher stiffness reduction, which was much more evident for the blend TB3, providing a value of only 36 MPa. It was pointed out that the stiffness moduli measured for AR dry were less delicate at high temperatures (> 30 °C). Hybrid fillers exhibited initial moduli of polymer nanocomposites that were much more eminent than composites with CB or only the nanofiller. By adding nano- Al_2O_3 to the NR matrix, the modulus of the nanocomposite was immensely heightened for NR/G nanocomposites, delivering an excellent modulus of 1.2 GPa. The storage modulus of NR/CNC nanocomposite with 2.5 wt% CNC was about 21 times higher than that of NR at 25 °C. Here, the 100% modulus in the direction was about 1.5 and 1.3 times higher than those in the transverse direction owing to the interaction of PMBMA-CA-NR, where the obtained modulus films were significantly enhanced⁷⁴. Feng et al. presented the dynamic complex modulus data of a 10% pyrolysis carbon black (PCB) modified binder and SK70# base binder⁷⁵. The moduli of both PCB-modified bitumen were higher than those of the base bitumen in both testing temperature ranges, and it was illustrated that the high-temperature deformation resistance of bitumen is improved with the installation of PCBs. The PCB-2 reinforced binder was found to have higher G values, and noted that PCB-2 improved the high-temperature deformation of bitumen greater than PCB-1. The results showed that the complex modulus was the highest (350 kPa) for the PCB-2 modified SK70# bitumen at 30–50°C, where it was 15–18 kPa at temperatures 50–70°C. There are several effects: the optimum time and scorch time were perceptibly minified using microwave treatment on GTR particles, resulting in the heightened modulus of materials and Young's modulus enhancing with the pic time and with the summation of clay. Another irrefutable panorama of GTR internalization into the epoxy matrix was the raised stiffness extracted by the compressive modulus. As the modulus was decreased

in the linear mode with microwave energy, the SEM-analyzed structure of materials revealed the detectable improvement of the port matrix and filler in the case of microwave-microwave-treated GTR⁷⁶. Nano- $\text{Al}_2\text{O}_3/\text{NR}$ nanocomposites were analyzed for the investigation of modulus in tire manufacturing by *Fu et al.*⁷⁷. They observed modulus increment by adding nanoparticles into NR. The modulus at 100% was decreased during engulfing in acid solution owing to the regular dampening of the intercellular substance resulting from the extensive root chain scission. However, when the nanocomposites were immersed in alkaline solution, the modulus level was negative at 100%, which resulted in a decrease in modulus⁷⁸. *Honorato et al.* screened out the elastic modulus as a function of temperature for the samples providing the cross-linking density⁷⁹. It has to be considered that the storage modulus in the glassy state (60°C) and at room temperature (25°C) was attributed to the cross-linking density and resulted in the same sequence: F3 > F4 > F4 > F1 > F2. Mono-sulfidic links were prevalent in formulations F3 and F4 under dynamic stress and stress. They turned less repellent, and thus, the compound F2 was vulcanized with the MBT/TMTD system and presented the moduli behavior that reasoned out the cross-link density⁸⁰. The storage modulus of H-1 and X-1 TPVs was the highest among all TPVs, indicating the constitution of the highest density of cross-links in the XHNBR and HNBR rubber phases. The storage modulus was decreased with decreasing the thermoplastic stage in the range of 50-30 phr, which resulted in the storage modulus of H-1 TPV to 367.3×10^2 MPa and the storage modulus value of H-3 TPV to 157.1×10^2 MPa. TPVs of 50:50 blends demonstrated the highest complex modulus, indicating the highest cross-link formation occurred in H-1 and X-1 TPVs. The complex modulus values of HNBR/PA12-based TPVs were partially higher than those of G^* of XHNBR/PA12-based TPVs. Consequently, the sample code X-1 released the largest modulus (100%) of 16.9 MPa than other TPVs. Again, the storage modulus of XHNBR/PA12-based TPVs (X-1, X-2, and X-3) was notable for their potential application in the automotive sector⁸¹. *Leng et al.* stated that the Log the Log DMT modulus-length curve demonstrated the entity of silica that ever crossed the BR the BR matrix/interface silica particles/VMQ phase/interface silica particles/BR matrix⁸². The stiffness modulus of bitumen after PAV was illustrated by the fact that the logarithmic creep stiffness modulus was decreased bit by bit with a time postponement in the constant force loading method. The largest slope of the creep modulus departed the strongest creep ability in the following order: original bitumen < SBS-modified bitumen < SBS/CRP-modified bitumen. The modulus of SBS-reinforced bitumen was nearer to that of the original bitumen at the same temperature. However, SBS/CRP-functionalized bitumen provided the strongest low-temperature relaxation capacity and better low-temperature crack resistance⁸³. *Li et al.* characterized the modulus ($G^*/\sin\delta$) of asphalt

pavement at high temperatures of different MACRMA samples⁸⁴. It was examined that the modulus gradually increased with the increase in loading frequency. All $G^*/\sin\delta$ values of modified asphalt at 0.1 kPa were insignificant between aged and immature asphalt higher than 1.2 kPa and became larger than 3.2 kPa when the reinforced temperature was 190 °C. The lowest $G^*/\sin\delta$ value was found to be 7.29 kPa when the MACRMA was at a premature temperature. The trends for the functionalized asphalts at different aging times revealed that $G^*/\sin\delta$ values of aging asphalt are heavier than 8.6 kPa, where MACRMA after 190°C aging conditions possessed the largest $G^*/\sin\delta$ values, reaching 13.37 kPa at 150°C or higher with the increase of loading frequency, which successively resulted from *Zhou et al.*⁸⁵. As the lower temperature enlarged the creep stiffness modulus and indicated the deformation resistance of asphalt, the m-value was decreased after UV radiation in the water medium⁸⁶. *Mostafa et al.* showed the stress-strain curvatures for SBR and NBR vulcanizing filled with several CB loadings at 25, 70, 100, and 125 °C⁸⁷. The stress-strain curves were obviously nearer to the filled compounds at different temperatures. The mechanical impact of CB loading on the 300% modulus of SBR and NBR vulcanizing effect was more vigorous due to the oxidative degradation formulated in short order in the loaded samples. Variation of the 300% modulus versus CB content for filled SBR vulcanizing screened out the lowest stiffness of 6-8 MPa against carbon black loading (70 phr) at 125°C, where it was close to 12 MPa against the same conditions. An illustrative dynamic stiffness was developed from the plot of storage modulus ($\log E'$) versus temperature that $\log E'$ was started from -60°C to 0°C, except that the modulus was remarkably unchanged by *Naskar et al.*⁸⁸. Moreover, the loss modulus ($\log E''$) plot showed an extensive maximum (a broad doublet peak) of the overlapped peaks against temperature. Initially, a small but sharp peak arose at -40°C due to NR, where the broad peak was attributed at -32°C for SBR. However, the desired peak for BR was not transparent in the DMTA curve perchance due to its low level in the mixing, which raised the degree of rubber-filler fundamental interaction to cause less extrusion. *Maharaj et al.* tested the complex stiffness (G^*) by adding 2% and 5% CR to TLA and TPB, respectively¹⁰³. It was indicated that TLA-modified CR performed the highest G^* values than TPB over the oxidation system, with stiffer and more elastic characteristics. The complex modulus was comparatively altered as a consequence of variant frequencies. The effect of the CR made it possible to create a stiffer TLA-reinforced material by the summation of 2% CR, where blending TLA with CR > 2% preferred a significantly stiffer and more elastic material. However, TPB functionalized CR and released a fringing increase in modulus.

2.3. Tensile Strength

In this case, the strength and FTFT results were bumped to be precisely equal as the tensile results were equal to the reasons owing to more filler-filler fundamental interaction compared to the virgin black⁶. The tensile strength was decreased for compounds comprising virgin black than those controlling renewed carbon black (24.5 MPa). *Susanto et al.* monitored the tensile strength of SBR/NR composites using RF-modified starch extracted from *Dioscorea hispida denses* (DRF) vulcanized with t90 at 150°C using hydraulic pressure³². The tensile strength was increased by adding filler due to the thermo-oxidative system. The loading over 25 phr or even more starch was used to neutralize the tensile properties, and an initial deterioration happened for SBR/NR/DRF composites owing to a tremendous post-curing effect, high crosslinking density, crosslink scission, stiffening effect, and severe oxidative degradation at higher temperatures. *Muller et al.* demonstrated the analysis of the tensile strength of a composite mixture, which evaluated the impact of different ratios of active rubber powder (ARP) on the adhesive bond strength³³. Although the tensile strength was decreased by adding ARP, this quantity reached higher strength (20–40%) than the composite with RP rather than the composite material with ARP. The results exhibited that the statistically nonhomogeneous tested composite materials ARP5 to ARP30 with matrix M let on to the laboratory environment and the influence of the cyclic degradation. The tensile value was smaller for the composite material ARP30, up to 74% of those discovered in the laboratory environment, and up to 70.5% for those exposed to the cyclic degradation ambiance. Conversely, *Dan et al.* analyzed the composition: 85% waste rubber + 5% coir fiber + 10% polypropylene was a strong reinforcement by increasing the tensile properties of the polymer³⁴. The plot of maximum stress (2.15 N/mm²) over the sample assessed the composition with CF 5%, which was the highest but ascertained to be decreased with the internalization of coir fibers due to lower stiffness and ductility. The tensile strength was monitored for the mixes containing L-cys and L-cystine dimethyl ester dihydrochloride (ELCH) *Debnath et al.*³⁶. *Ahmed et al.* observed the tensile strength by the addition of marble sludge (MS) into natural rubber dependent on filler loading³⁹. The tensile of MS powder-filled NR complexes with several micro-size corpuscles (10, 20, and 75 µm) observed that at 70 pphr, the NR composite conformed to 10-µm MS particles exhibited a maximum peak of 11.65 MPa, which was 230% higher than that of the unfilled NR composite owing to the filler-rubber interaction. Therefore, the smaller micro-sized particles of MS (10 µm) possessed greater tensile strength than the larger ones (20 and 75 µm) in NR composites. This was due to the high dissemination and the fundamental interaction of small micro-size molecules of MS in the NR phase. *He et al.*⁴⁰ evaluated the physico-mechanical properties: the tensile strength of natural rubber and thioglycolic acid functionalized natural rubber

(TGA-ELMWRN) occupied with mixtures of carbon black and carbonized rubber seed shells (CRSS) were inquired as a function of different filler compositions⁴⁰. The tensile strength varied from 16.8 MPa for mix A to 8.3 MPa for mix I, demonstrating a 50.6% decrease in tensile value from 100% CB to 100% CRSS. As the concentration of CRSS in the blend increased, the tensile strength was reduced. The functionalization of pyrolysis carbon black impacted the partial change in the tensile strength demonstrated by Delchev et al.⁴³. The tensile strength values for vulcanizing modified pyrolysis carbon black were increased. *Ismail et al.* marked the tensile strength (TS) (12.8 to 6.7 MPa) with 4–6 phr of peroxide concentration of the HNBR and XHNBR compounds for the development of TPVs⁴⁵. They studied the mechanical features of thermoplastic vulcanizing (TPVs) were diminished with decreasing PA12 in the range of 50 to 30 parts. Here, V₅₀P₅₀PE₄ TPV exhibited the highest strength (18.5 MPa), and V₇₀P₃₀PE₄ TPV delivered the lowest tensile strength of 9 MPa. These typical values were altered due to the concept of recycling the TPVs, where the rubber level softened much more than the plastic (PA12). The EPDM-r specimens were investigated, and it was determined that EPDM-r 30 was larger than that of the controlled sample by *Zanchet et al.*⁴⁹. According to the procedure, the higher the EPDM-r UV content, the higher the tensile strength. Thus, the value of EPDM-r was found to be highly active at 30 phr. The tensile value was altered with changes in the proportion of N550 and rCB in the scheme checked by *Sagar et al.*⁵⁰. They observed the tensile values in the range of 9.6–5.9 MPa for the increment of rCB. The rubber reinforcement with carbon black was responsible for the weak interaction in the region of rCB. *Poikelispaa et al.* observed the tensile strength of MWCNTs at 5 phr, where the property started to fall due to insufficient dispersion of MWCNTs⁵¹. However, the larger the surface area of MWCNTs, the larger the tensile strength appreciated, likened to the compound fitted only with CB, and as luck would have it, the MWCNTs are well dispelled. The 12% WTR+4% APAO modified asphalt mixture showed the largest tensile stability rather than the modified asphalt mixture: 12% WTR+4% APAO showed the largest tensile stability with high-temperature performance evaluated by *Yan et al.*⁵³. The synthetic giant tires were characterized by using blends of natural rubber (NR) and brominated butyl rubber (BIIR), following tensile strength (18.8–12.0 MPa) values widely varied, which were evaluated by *Motar*⁵⁵. The collateral tensile strength seemed to be conducted, and the tensile strength of CRM mixtures under stationary or recapitulated compressive loads by *Hassan et al.* measurement of the horizontal displacement reaction to compute the horizontal tune checking of the load enforced parallel to the vertical skin of the specimen⁵⁷. The corresponding horizontal strains showed a significant increase in strain potential at low temperatures for tire manufacturing. *Zedler et al.* investigated all tested samples in the 5.2–6.1 MPa

range and denoted the sample correlational statistics and tensile properties of reclaimed GTR⁶³. Again, the cross-linked GTR particles with elastomeric chains in the samples explained the partial divergences in the tensile properties celebrated for rectified GTR. The tensile characteristics that prevailed in reclaiming GTR were likened to other reclaimed rubbers. The results preferred that the reclaimed GTR tensile strength presented a 3.2–8.4 MPa mutation. It was concluded that a part of the reclaiming method and GTR characteristics colligated with curing conditions strongly impacted the target functioning properties of reclaimed rubber. The tensile strength of the tire rubber compound was found to be 145.5 kg/cm² and 128.5 kg/cm² for the v-belt rubber compound demonstrated by *Singh et al.*⁶⁵. Again, the tensile strength of the tire rubber compound was greater than the v-belt due to the greater amount of rubber processing oil, sulfur, and antioxidants added to the composition. *Kirushanthi et al.* developed and evaluated the tensile strength of rubber composites modified with tire waste and amorphous silica⁶⁶. The rubber, crumb rubber, and silica were merged in various quantities to acquire optimal tensile strength. It was displayed that the increment of crumb rubber decreased the tensile strength with increasing crumb rubber. The strength was marginally increased with the adjustment of the carbon black matter. As the carbon black was added to the D-GTR/virgin blend compounds, suppressing the rubber cross-linking quality, the material's tractability was reduced. The tensile properties were deteriorated by the accession of the D-GTR compartmented to the master compound for several reasons, like cross-links of the D-GTR, inhomogeneity in the blend, and migration of curves between the blend phases in the whole tire material, as shown by *Habibah et al.*⁶⁷. The tensile strength of a typical tire tread compound with various contents of D-GTR exhibited that the adjustment of carbon black values was larger than the virgin tire tread and without adjustment of carbon black. Despite the tensile strength values being lowest for those compounds having high bromobutyl contents, it showed an improvement in air retentiveness having high bromobutyl contents. *Liu et al.* studied the dynamic loss (Tan δ) and compression heat generation of the blend rubber, where the tensile stress was decreased by 100% and 300%, but the tensile strength changed due to temperature impact⁶⁸. It was seen that the tensile strength value of the DPG-cured compound was the highest, providing additional crosslinking espies. Mixing 5 mentioned the highest tensile, about 20.15 MPa, obtained from only pure CBS-cured compound without any DPG compared to others. Moreover, the tensile strength was decreased by ~35%, and it was noted that the retentiveness of the tensile strength was found to be maximum for compounds cured with only CBS. The determination was to investigate the consequence of a maleimide curing system on the tensile property of the ground tire rubber and waste polypropylene (GTR/WPP) blends *Egodage et al.*⁷⁰. The variation in tensile

strength with HVA-2 subjects to coalesce with and without DTBPIB showed that the strength was increased initially with HVA-2 level at 4 php, and a 33% increase in tensile strength over the control blend was detected. Moreover, the rough failure surface was responsible for better tensile properties, where the 3H/0.6D blend exhibited a comparatively higher tensile strength (18 MPa). *Feldman et al.* evaluated the strength of a natural fibril silicate, NR/polygorskite, and developed parameters to reduce the agglomeration of the nanofiller⁷⁴. SEM and AFM deduced an outstanding characteristic between NR latex and peeled-off (NaCMMT/polyethylene imine-g-polymethyl methacrylate) (NaCMMT/PEI-g-PMMA) particles drawn as its strength increased by 85% with 10 phr. The tensile was found to be 48 MPa, associated with high nanofiller content nanocomposites that markedly increased with the filler, dictating a potent reinforcing effect on NR. NR was reinforced with nanoaggregates, demonstrating very good tensile due to nanofiller elastomer activity and the complex impact of the NR-protein scheme. The highest strength was attained for the crosslinking NR/NaCMMT. *Formela et al.* reported microwave treatments in the recycling of waste rubber⁷⁶. SEM images were performed at the active site of ultrasound-treated rubber, and the fracture surface of LDPE/waste rubber composites was found, which resulted in the best tensile range. Here, the GTR particles were increased with microwaves, were effectively modified, and led to the 49% increase of tensile strength compatible with NR/GTR composite filled with unadapting particles owing to the increased roughness and specific surface area after treatment, which raised the characteristic between phases. The consequence of treatment was stronger in the consequence of GTR in truck tires due to higher content of NR and higher degree of de-vulcanization. *Fu et al.* exhibited the reinforcement impact of Al₂O₃/NR nanocomposites. The stress transition caused by tensile crystallization developed the compatibility and attraction between the filler and NR, resulting in magnificent tensile strength⁷⁷. On the other hand, the tensile strength started to diminish at higher filler content due to the accumulation of nanoparticles. However, the tensile was significantly positive at 3-5 phr. The tensile strength of asphalt functionalized rubber was decreased by the number of thermal cycles observed by *Othman*⁸⁰. This carried interfacial durability between the binder and the aggregate due to the power of rubber to enhance the adhesive agent between aggregate particles and asphalt cement. The NR/RGTR-4 blend exhibited less amount of tensile strength (19.34±0.60 MPa) for the poor dispersion and weak interfacial adhesion between the GTR particles and NR matrix by *Zhang et al.*⁸⁶. It was due to the approximately cross-linked network of the gel fraction of RGTR-4 and substantial interfacial adhesion between RGTR-4 and NR. As the tensile strength of vulcanizing filled with increasing RGTR content was 10-40 wt% conceitedly that of the NR vulcanizing, it was followed from 18.5±0.49 MPa

to 11.4 ± 0.25 MPa increased in the range of 40-70 wt%. Additionally, both H1 and X1 exhibited remarkable tensile due to cross-linking, where HNBR/PA12-based TPVs decreased in the 19.1-13.5 MPa range. *Naskar et al.* followed the physical properties of ground rubber tire (GRT) filler NR compounds⁸⁸. Here, NR was mixed with GRT of <52 mesh particles, which registered a 71% retention of tensile strength, while the equal quantity of natural rubber amalgamated with GRT of 100-150 mesh particles and demonstrated 31% retention of tensile strength. However, compound D delivered the highest tensile, 8.0 MPa, for the GRT-filled NR compound. The mechanical properties were measured at a higher strain level, which caused a larger worsening in the tensile strength of the cords⁸⁹. *Nuzaimah et al.* monitored the improvement of tensile strength by acrylonitrile butadiene rubber glove waste blended epoxide natural rubber (ENR 50)⁹⁰. Here, the addition of SBR scraps demonstrated the best tensile in the condition of SBR virgin without SBR scrap due to the interfacial adhesion but partially decreased at 40 phr of loading NRP. On the other hand, the latex waste additive enhanced the strength of this rubberized compound. *Xiong et al.* investigated the impact of

styrene-butadiene latex (SBL) on the potency of the rubber-cement matrix for automotive purposes. Since the combined efficiency of the interfacial adhesion depended upon the SBL content, fluoro rubber (FPM) exhibited the best tensile strength between rubber and cementations paste except for the maxima exhibition for acrylonitrile-butadiene rubber (NBR) and natural rubber (NR)⁹¹. The authors investigated the strength value of the NaOH treatment, except for H_2SO_4 and $KMnO_4$, which modified the hydrophilic nature of rubber crumbs and raised rubber-polyester interfacial adhesion. Hence, the tensile strength of the composite was increased by 2% from the untreated rubber. The correlation revealed that the NaOH treatment provided the highest value of 9.5 MPa, and this finding could prompt many attempts to reprocess waste rubber to battle environmental troubles affecting a large amount of waste rubber and therefore heightening the composite strength^{92,93}. *Kushwaha et al.* focused on developing high-tensile reclaimed rubber by partially substituting virgin rubber. Here, the sulfur concentration affected the mechanical behavior of the reclaim better than the control NR compounds⁹⁴.

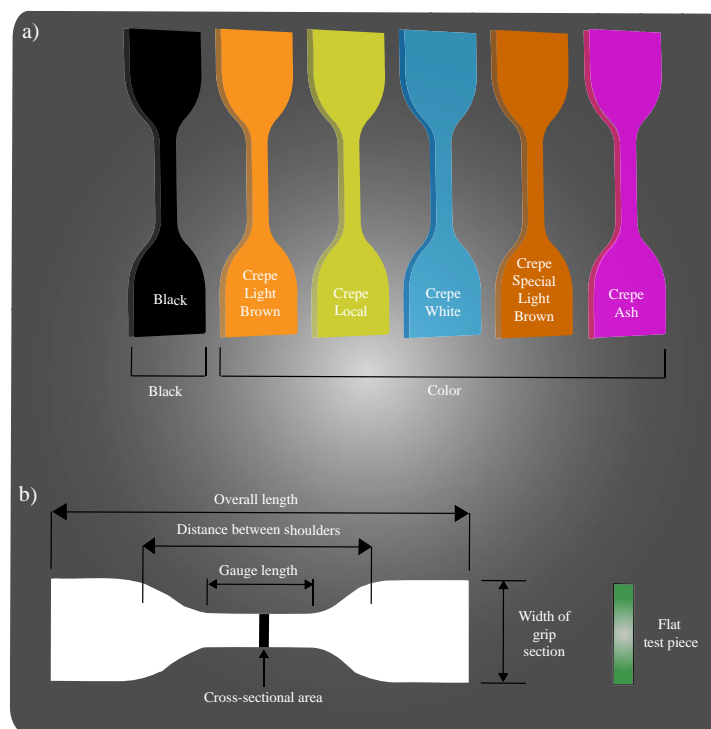


Fig. 4. The tested rubber specimens' shape for mechanical characteristics

The strength evaluation of six different compositions: 0, 20, 40, 60, 80, and 100 phr of CB with NR/BR/SBR rubber blend was found by *Jovanovic et al.*⁹⁵. The strength was diminished against oxidative conditions. Besides, the strength was increased as a consequence of cross-linking. It was demonstrated that the findings were highlighted by CB content, where the largest value (17 MPa) was for NR/BR/SBR/CB samples containing 80 phr of filler. *Motiee et al.* monitored the

accuracy and precision of the BR/SBR blends, in which the passable strength value was 0.93 with a correlation coefficient⁹⁶. The UV intervention of crumb rubber bestowed little to enhance the strength, with an intermediate strength of 3.3 MPa, where the sulfuric acid-treated crumb rubber aggregated. It showed a larger improvement in the E value of 2 GPa, as determined by Alawais et al.¹⁰⁰. The strength increased to 13 MPa owing to the addition of

limestone by-product aggregates. *Bandyopadhyay et al.* measured the tensile strength, which diminished as the quantity of regenerated black was enhanced. *Zhang et al.* were established to show the stress-strain curves for GTR-filled EPDM complexes, in which the unreacted GTR-filled composites assessed the strength of 0.27 MPa¹⁰⁵. Alongside the vulcanized GTR-filled EPDM, it was potentially raised to 0.72 MPa after pan-milling for 20 cycles. Therefore, the tensile was heightened by 166.7% more than the various tested samples for mechanical stressing (Fig. 4).

2.4. Elongation at Break

The extension breakdown decreased for virgin black, as illustrated by *Bandyopadhyay et al.*⁶. The 50% regenerated black compounds released the highest amount of extension (417%) under normal and oxidative conditions. *Susanto et al.* observed the tensile property: elongation at break went through diminishing scope by the longer oxidative evaluation³². A marked elongation at break possibly caused the impairment of SBR/NR/DRF composites. It was noticed that the elongation at break was evaluated as the lower value following the oxidation time. A small and remarkable elongation at break assessment was inserted in a mixture of L-cys and ELCH, where a little deviation was displayed only at the high elongation observed by *Debnath et al.*³⁶. The statistical average compounds concerning a bombastic elongation at break (305%) of DPG vulcanized compound (mixture 6). The elongation at break was reduced by incorporating MS waste into the NR composites checked by *Ahmed et al.*³⁹. The determined extension results were fixed at 70°C and 100°C. Although the results showed that the NR composites filled with different micro sizes of MS 10 particles possessed the largest extension at 100°C, the elongation (958%) was increased at 70°C. Here, the elongation at break was found to be a reduced value of 18.6% from mixture A to mixture I noticed by *He et al.*⁴⁰. However, the highest value of 985% elongation was studied for mix A, and the lowest value of 801% was identified for mix I, which implied that the carbonized rubber seed shell (CRSS) had not raised the elongation of the vulcanizing. *Delchev et al.* monitored the elongation at break, which decreased with the increase of pyrolysis carbon black⁴³. It was less than 10% for vulcanizing virgin and reinforced pyrolysis carbon black of 50 phr rather than 70 phr. The remainder of the elongation decreased with increasing pyrolysis carbon black. Although the values of the elongation break and residual elongation were marginally lower due to low ash contents in the modified pyrolysis carbon black, the lowest elongation values were the device characteristic of all compounds having silicon oxide. V₅₀P₅₀PE₄ TPV showed an extension of 123%, whereas V₇₀P₃₀PE₄ TPV possessed the highest value of 76% with decreasing PA12 content from 50 parts to 30 parts because of the info that after reprocessing the TPVs at 70 phr of AEM assessed by *Ismail et al.*⁴⁵. V₅₀P₅₀PE₄

TPV preferred a minute growth in elongation at the break due to the lowest rubber divide among all TPVs. *Fazli et al.* showed the largest extension values (20%). Still, the cross-linked structure of the GTR particles and poor adhesion with the PP matrix assessed the low value due to crack initiation and rapid crack propagation⁴⁶. Additionally, the oxidative system of GTR raised the mechanical property of HDPE/PE-gMA/GTR compounds, where the extension was found to be about 24% for all blends with different reinforced rubber particle sizes. The result evaluated that the elongation at break of HDPE/GTR/POE (60/20/20) compounds was 129%, larger than 82% for HDPE/GTR/EVA (60/20/20) compounds. Moreover, the presence of RR short chains and processing oil raised the elongation at the break of RR compounds due to a plasticization effect, where the cross-linked gel part of recycled rubber particles increased the rubber concentration of gel content in the blends, leading to increased crosslink density and thus producing lower elongation. However, the optimum vulcanization time was obtained for the maximal elongation at break (57%) for these tested samples. *Ramarad et al.* investigated the extension of rubber blends containing ground tire rubber/reclaimed tire rubber (GTR/RTR) into the NR, NBR, and SBR⁴⁸. The reason was noticed for the deterioration of EB in the NR blend due to the less homogenous blend. Besides, the GTR/RTR content was raised with the gel content in the ground substance, which resulted in lower EB. The EB was trusted to be improved owing to the plasticization characterized by the processing oil present in GTR/RTR. Several potential data for SBR/RTR were collected, where the values of EB improved by 12% compared to SBR/GTR rubber blends. The regular kinship of thermoplastic blends with increasing GTR/RTR depicted the shortage of EB in blends at higher loadings of GTR/RTR, where allylamine-reinforced GTR via UV discussion ameliorated the EB by 7% in the PP/GTR blend. Nevertheless, substituting PP with MAgPP afforded substantial improvement in EB. Finally, the RTR blends were expected to extend better elongation at break compared to GTR blends, which will be engaged in contrasting and comparing the GTR and RTR blends to cover the deficiency in EB of GTR blends. *Zanchet et al.* described that the EPDM-r content was intended to diminish the extension break of the samples and decrease the amount of raw EPDM in the blends⁴⁹. Besides, this elongation value was reduced due to the high cross-link density and the release of the processing oil from the EPDM-r UV. In this case, the elongation at break was found to be above 280% for EPDM-r UV 20. Peroxide cross-linked AEM compound V2 showed elongation at a break of 643%, drastically reducing it to 206% for the V6 compound. *Sagar et al.*⁵⁰ introduced the potency of filler loading on the extension break⁵⁰. The plot exhibited that the elongation was enhanced when rCB was added in the experiment, in which the EPDM vulcanizing with N550 increased; the elongation was 210%, and the value was reached at 390% for the

system with only rCB. Since SEM implied that the N550-filled EPDM with rCB affected the elongation at the break of the compound, it decreased fractionally from 390% to 367%. *Poikelispaa et al.* monitored the highest MWCNTs supposed to increase the polymeric interaction, which results in the increment of elongation at break compared to the chemical compound fitted only with CB. As luck would have it, the MWCNT is well-diffused⁵¹. The elongation started to decrease for the exceeded amount of MWCNTs (>5 phr) due to the inappropriate dispersal of MWCNTs from the rubber matrix. *Motar et al.* potentially characterized the elongation at break (510–600%) for high contents of bromobutyl compounds⁵⁵. *Singh et al.* showed that the tire rubber possessed 400% elongation compared to the V-belt rubber, which possessed 210%⁶⁵. *Habibah et al.* investigated that the elongation at break of a passenger car tire tread compound was decreased with increasing content of D-GTR of up to 50 phr due to the homogeneity in the blend and movement of curatives and taints in the raw material of the DGTR⁶⁷. *Liu et al.* tested the largest extension (300%) of waste tires⁶⁸. The experimental study visualized that only the extension was increased when the compressed heat generation of the rubber blends was manifestly trimmed down. It was clear that the fixed percentage elongation stress (449/73) of amalgamated rubber significantly decreased by 100% with the rise of the amount of carbon black added to the rubber in

the transition layer of the all-steel load radial tire. Elongation at break was raised with N, N'-meta-phenylene dimaleimide (HVA-2) using a laser extensometer by *Egodage et al.*⁷⁰. Moreover, the addition of di(*tert*-butylperoxyisopropyl) benzene (DTBPIB) was preferred to increase the elongation at break markedly for all HVA-2 levels examined. An optimum value was observed at the 3 phr level of HVA-2 due to the extra cross-linking organized in the GTR phase. However, the maximal increase in extension break over the control blends (210%) was observed at 0.6 phr DTBPIB with 3 phr HVA-2. *Formela et al.* studied the vulcanized crumb rubber by investigating the elongation at break at 10 and 20 wt% material contents⁷⁶. The mechanical properties of the studied materials showed that the SBR scraps led to an increase in elongation at the break due to the partial degradation of the polymer main chain. *Fu et al.* investigated the extension effect of nano-Al₂O₃/NR nanocomposites on filled NR vulcanizing⁷⁷. It was noticed that the elongation at break was increased and then decreased with adding filler content, but it delivered an optimal value (730%) at 1 phr filler content. Again, the tested material proposed the improvement of elongation after acid and alkaline tests owing to the increase in crosslink density. The physico-mechanical behavior of the peroxide-cross-linked HNBR and XHNBR gum compounds was studied by *Ismail*⁸¹.

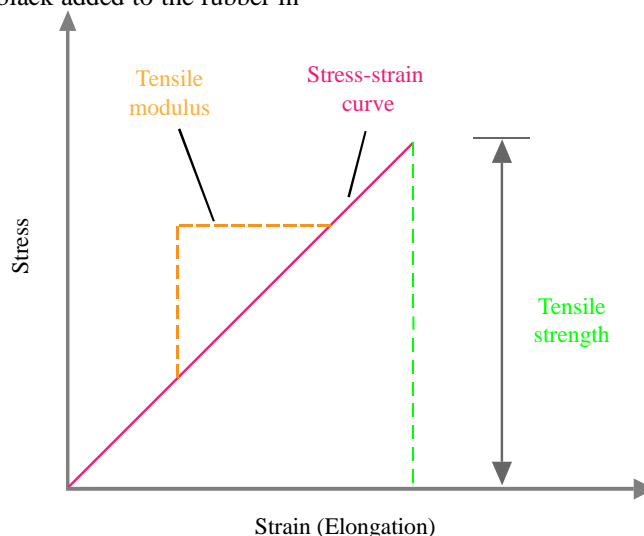


Fig. 5. The plotting principle of mechanical features for tire manufacturing

It was visualized that the level of %EB of the gum compound was reduced at 6 phr of peroxide. The extension percentage of the HNBR gum compound was drastically reduced in the range of 1013–508% with increased peroxide concentration within 4–6 phr. The equal half blend ratio (H1:X1) of thermoplastic vulcanizing (TPVs) exhibited the potential %EB based on mechanical properties regarding hydrogenated acrylonitrile butadiene rubber (HNBR/PA12) and partially hydrogenated carboxylate acrylonitrile butadiene rubber (XHNBR/PA12), owing to the largest cross-linking in

the rubber chemistry. It can also be mentioned that the extension was reduced from 197 to 128% for HNBR/PA12-based TPVs since the PA12 quantity was decreased from 50 to 30 phr. Although there was no axiomatic change with the fluctuation of VMQ minimal, *Leng et al.* significantly kept up the %EB of silicone/butadiene rubber composites (VMQ/BR) of 20/80 proportion⁸². The devulcanized GTR-EPDM (100/20) composites were plotted in Fig. 5 by *Zhang et al.*⁸⁶. The immature GTR-filled composites had 290.7% elongation. The elongation at break of the

devulcanized GTR-filled EPDM composite foam was potentially increased to 748.2%.

The elongation at break was tested by *Mostafa et al.* for SBR and NBR vulcanizing filled with several CB loadings at room temperature⁸⁷. The impact of CB loading on the elongation at break under oxidative conditions illustrated the degradation. The elongation at break values was decreased with stiffening. The elongation at break for ternary NR/BR/SBR (25:25:50) rubber blends with 100 phr of CB nanoparticles was reduced much more than other samples demonstrated by *Jovanovic et al.*⁹⁵. This is due to the degradation process of cross-linked materials and the reduction of polymer molecular weight for breaking the elementary chains. It was revealed that the elongation break was found to be about 340% at 40 phr content of CB.

2.5. Aging

Bandyopadhyay et al. characterized the stimulated aging nature of regenerated black compounds as somewhat improved compared to the virgin black compounds, in which the regenerated black compounds did not potentially develop with the accession of Si-69⁶. The mechanical properties, such as elongation at break, tensile strength, and modulus, were found to be decreased by the longer aging time. By the parameter, *Susanto et al.* imported the thermal oxidative-aging SBR/NR/DRF composites at 70 °C with different timing³². The impact of aging was depicted along with the loading of DRF on the aging of NR/SBR composites, and the longer aging time stimulated the cross-linking in the rubber matrix by decreasing the average molar mass of the SBR/NR chain between adjacent cross-link points. The age-resistant nature of vulcanizing obtained from the binary combination of amino acid L-cystine (Lcys) and its derivative L-cystine dimethyl ester dihydrochloride (ELCH) with accelerators like N-cyclohexyl-2-benzothiazole sulfenamide (CBS) tricked out by *Debnath et al.*³⁶. The combination was aged for 72 h at 100 °C in a forced air circulating oven for the aging experiment to establish the mechanical features. Moreover, the Payne effect extended a lower storage modulus value at low strain due to the less filler-filler interaction of DPG along with CBS at 1 phr ELCH. *Lee et al.* assessed the mechanical images of poly-ketone fiber. They considered themselves a reinforcing stimulus of mechanical rubber goods (MRG) to aging conditions, which were very crucial due to thermal and humidity aging³⁷. Thermal aging at high temperatures was largely caused by the rubber composite more than by humidity aging. Besides, the interfacial adhesion of the poly-ketone/NR composites was monitored by the primer therapy that was exerted in aging conditions. Consequently, the rubber hardness of the poly-ketone/NR composite was heightened with increasing thermal aging time because of the oxidative system and the cross-linking reaction of the rubber matrix. Alongside, the oxygen content of the NR matrix was increased with the

thermal aging temperature and time owing to the surface oxidation at an elevated temperature. It was clear from SEM that the interface was changed surface by thermal aging because of the oxidation and hardening of NR. *Wright et al.* suggested tire models under specified aging conditions, providing the essence of a tire's age on the execution nature of a tire, such as vertical, longitudinal, and lateral modulus, which were not well explored³⁸. Since a tire was artlessly aged and tested periodically during aging, the stiffness curves covered the framework parameters. Generally, these aging effects were outperformed by testing an instrumentation threshold of about $\pm 1\%$, which was not considered unimportant. Three different microsized, 10, 20, and 75 μm with five different grounds of loading up to 90 pphr were employed in NR composites with MS loading on the mechanical properties tested by *Ahmed et al.*³⁹. The relaxation of thermal aging at 70°C and 100°C for 96 h has also been studied in the NR composites. It was clear that the aging of NR was complicated. Still, the thermally aged counterparts had been appraised and equated to one another by the effect of temperature on the aging property. The aging characteristics of natural rubber functionalized blends and thioglycolic acid-reinforced epoxide low molecular weight natural rubber (TGA-ELMWNR) filled with a mixture of carbon black and carbonized rubber seed shell (CRSS) in modified chemicals were investigated by *He et al.*⁴⁰. They fixed that mixture G (50% CB: 50% CRSS) possessed a synergistic aging effect on both CB and CRSS. Besides, the detected development suggested CRSS imported a positive aging shape in rubber vulcanizing, and consequently, CRSS was utilized in tires. *Buhlmann et al.* examined the tire/road resounding mensuration with the proximity (CPX) method, and the tire aging was accompanied by noise emission properties⁴². These aging effects were required when the individual tires were supervised over the fourth dimension. The investigation of the aging process of the new reference-tied SRTT and Avon AV4 suggested that tire aging was a primary factor when tire/road noise mensuration was carried out by using the CPX treatment. The oxidative evaluation indicated that the mechanicals on in-service tires possessed a greater degree than the standardized operation. The aging constants of SBR altered vulcanizing, controlling the minimum add-up of virgin and modified pyrolysis carbon black, were developed in and out of heat aging by *Delchev et al.*⁴³. After completion, it was obvious that the adjustment of pyrolysis carbon black affected the heat aging of SBR-based vulcanizing, and hence these compounds showed more aging resistance where the reinforced pyrolysis carbon black had an excellent impact on the heat aging of the vulcanizing. The thermal short- and long-term aged features of SBR and NBR composites were investigated by *Choi et al.*⁴⁴. The thermal aging altered the activation energy for the crosslink density, which was attained from the Arrhenius plot and aging variation to normalize the aging features of SBR and NBR. It

resulted that the crosslink density gained the lifetime of t50 and t100, respectively, at 25.8°C, where the NBR had much more thermal resistance than SBR owing to the decelerating consumption of anti-degradation that stayed on in the samples by thermal aging and bar abjection of the rubber chain by a phenyl or nitrile group. Besides, the allylic proton entity of the SBR was larger than that of the NBR by about 1.4 times to take part in the crosslinking reactions of SBR, which could be more eminent than NBR. The ethylene propylene diene monomer rubber (EPDM) industrial waste was aged through ultraviolet radiation (UV) in a UV chamber conducted by Zanchet et al.⁴⁹. It was shown that the aging of the waste for 156 h did not induce an austere erosion system owing to the highest molecular hardness of the samples. Poikelispaa et al. carried out the aging to examine the ensuing effect of the internalization of MWCNTs in the rubber matrix⁵¹. Although MWCNTs replace the CB, the average value of the slope was found to be approximately 0.84 due to cross-linking. The results revealed that the aging of MWCNT/CB-filled NR/BR entities at 70°C is mastered by the constitution of crosslinks, not by destructive degradation of the bonds. Boruta et al. investigated the aging effect of crushed rubber powder as filler content for rubber-manufactured compounds on vulcanizing ozone⁵². The deterioration effect was observed in lower powder concentrations than in the ozone aging of rubber. 15% WTR + 4% APAO modified asphalt mixture largely visualized the best anti-aging performance by Yan et al.⁵³. The crumb rubber reinforced asphalt (CRMA) performs better than matrix asphalt (MA) in road engineering. Carvalho et al. stated that aging under aerobic conditions increases the total quantity of crosslinks: mono-, di-, and polysulfide crosslinks⁵⁴. Ali et al. also studied the crumb rubber modifier concentration on the mechanical features of rubberized bitumen after aging tests had been conducted using short-term aging (i.e., rolling thin film oven test or RTFOT) and long-term aging (i.e., pressure aging vessel or PAV)⁵⁶. It was examined that the aged rubberized bitumens were about 36% and 44% for rubber contents of 8% and 16% under RTFOT conditions, while the increased PAV aging values were about 78% and 82% for rubber contents of 8% and 16%, respectively, owing to the lower penetration aging ratio, which reduced the aging unit of rubberized bitumen binder. The blended rubber was observed by Liu et al. to evaluate the aging resistance⁶⁸. Mechanical properties: elongation at failure, hardness, and tensile strength did not alternate significantly between before and after aging. Owaid described the impact of aging on asphalt rubber as being developed by reclaimed rubber tires (0.5 and 1.0%) handled with anhydrous aluminum chloride (0.06, 0.12, 0.25, 0.5, and 1%)⁶⁹. The functionalized asphalt specimens were subjugated to aging. They did not allow significant changes because they resisted large stresses and cracks, ensuring a farsighted aging-linked lifetime. Feldman questioned the aging of NR/butadiene rubber

(BR) poly-blend tire tread compounds by the antiphony permutation of CB by MWCNTs⁷⁴. The outcomes have exposed the aging by using thermal stability and its application. Feng et al. used pyrolysis carbon black (PCBs) from the waste tires⁷⁵. In this case, the thin film oven (TFOT), pressurized aging vessel (PAV), and natural aging (NA) were explained by both the thermal- and photo-oxidative aging of the PCB-modified bitumen. It was normal that PCB-2 was found to be more positive in mending the photo-oxidative aging of bitumen than PCB-1. Both PCB-1 and PCB-2 modified bitumen exhibited the largest PRR values after all aging procedures, in which the PCB functionalized bitumen possessed better-aging resistance than the base bitumen. Fu et al. demonstrated the aging properties of alumina/NR nanocomposites⁷⁷. The aged Al₂O₃/NR nanocomposites exhibit an increase in tensile strength and a decrease in elongation at break after aging. The decrement in the tensile strength of unfilled NR with aging is caused by the regular weakening of the matrix, which results from the extensive main chain scission. In this case, the modulus and hardness of unfilled NR were raised and still lower than those of the aged nanocomposites, and it was possible after aging treatment. The nano-Al₂O₃ compiled with 1-7 phr filler content to enhance the tearing strength increases significantly at 1-7 phr filler content for both the unfilled NR and the nano-Al₂O₃ nanocomposites. On the other hand, the free radicals associated with the Al₂O₃ nanoparticles improved the thermo-oxidative aging resistance properties of the samples. When the Al₂O₃ nanoparticles became more than 3 phr, the reunification of Al₂O₃ nanoparticles was increased as Al₂O₃ nanoparticle content was increased, which would increase the percolation of oxygen and drive the thermo-oxidative aging feature of the samples. Then, the heat was prone to dispel the high thermal conductivity of Al₂O₃ nanoparticles developed by the aging of NR nanocomposites. The vulcanized natural rubber (NR) composites with accelerators in EV cure systems were investigated concerning the resistance to aging by Honorato et al.⁷⁹. They observed four NR formulations were made when posited to accelerate aging. There are two root aging processes, oxidation and ozone, which demonstrated that the most stable curing system had been utilized or that a more substantial quantity of crosslinks had constituted to improve these features in tires. Othman studied the high-temperature cyclic aging of rubber-modified asphaltic mixtures to improve the fracture resistance of the mixture at both low and high levels of thermal cycling in rubber and the fracture resistance of the mixture⁸⁰. At high temperatures, the rubber modifier increased the mixture's viscosity. Hence, it increased the adhesive bonding for asphalt cement and aggregate particles that can be conducted to imply the mixture's fracture resistance. Ismail et al. assessed the oil aging behavior for enriching high-performance thermoplastic vulcanizing (TPVs) that provided the dynamic vulcanization process in which the exclusive cross-

linking of the elastomer diverted into a significant improvement of the heat due to the formation of the highest mesh of percentage retention of TS, %EB, and hardness; shore (A and D) of the blends⁸¹. Alongside polar groups in rubber, polarity was inflicted, which was responsible for the oil resistance of HNBR and XHNBR. The silicone rubber (VMQ: 20/80) was combined with BR to improve its anti-aging properties, evaluated by *Leng et al.* through AFM and TEM to put on phase morphology of the VMQ-silica master batch/BR⁸². The concomitant crosslinking of rubber chains had happened, which resulted in the increment of TS and the decrement of EB owing to the aging: the action of heat and oxygen. After all, under the consideration of non-antioxidants, VMQ could also immensely heighten the thermal oxidative aging of BR composites. The one extended because of its better aging, leading to the extremely saturated Si-O-Si structure. *Akinlabi et al.* studied the temperature sensitivity parameters of Styrene-butadiene-styrene polymer/crumb rubber powder (SBS/CRP) modified bitumen⁸³. It was pointed out that the SBS/CRP-functionalized bitumen had a powerful anti-aging capability after long-term aging because of excellent low-temperature relaxation and low-temperature crack opposition. Besides, the ductility was decreased with long-term aging, as the softening point of SBS/CRP-modified bitumen did not drop significantly. It was obvious that the SBS/CRP-modified bitumen possessed an excellent anti-aging property after long-term aging. The stiffness modulus of the original bitumen was increased after short-term aging. In contrast, the SBS-modified bitumen and SBS/CRP-modified bitumen decreased due to the original bitumen intended to be in compaction during thermal-oxygen and pressure aging. *Li et al.*⁸⁴ visualized the effective thermal oxygen aging permutations of microwave-activated crumb rubber-modified asphalt (MACRMA) to investigate the shape of several aging components on the ownership of MACRMA. The linear fit analysis revealed that the correlation coefficient between the softening point values and aging time was 0.990. Usually, it could be realized that the softening point of the MACRMA was increased with the aging temperature and time increase, where the penetration and ductility gradually decreased. Accordingly, it could be that TFOT aging would increase the aging degree of leaching, regardless of aging time and temperature. The aged MACRMA was broadly reduced as the aging time was increased under the stress of 100 Pa with immature asphalt. For instance, the immature asphalt at 50 times was 29.52%, while the gradual strain of aged asphalt was less than 20%, indicating that the anti-deformation ability of MACRMA was increased. The aging prospectus of CRMA intact by microwave-activated crumb rubber and the aging mechanism of microwave-activated crumb rubber modified asphalt (MACRMA) narrated by *Zhou et al.*⁸⁵. It was

exhibited that MACRMA enabled the best anti-aging among them and the order: MACRMA > CRMA > MA. The large molecular size (LMS) of rubber asphalt bit by bit heightened the step-up of aging due to the quantitative characterization of the anti-aging degree of rubber asphalt materials, and the exponent of MACRMA was increased with the aging. This mechanical feature of the rubber composites containing reclaimed rubber was characterized by *Zhang et al.* and evaluated by accelerated thermal aging tests⁸⁶. The reclaimed rubber attained some active cross-linking bonds during aging. The structure was responsible due to the presence of oxygen during aging. Excellent aging resistance of the anti-aging agent and CB in the waste tires induced and reduced the thermo-oxidative aging reaction. Moreover, the anti-aging of RGTR finally influenced the use of antioxidants that might be boiled down or even fully ejected if RGTR participated in product preparation. *Mostafa et al.* executed the thermal aging treatment under the effect of temperature on the mechanical properties of styrene butadiene rubber (SBR) and nitrile butadiene rubber (NBR) compounds filled with different carbon black (CB)⁸⁷. Consequently, both the 300% modulus and the elongation at break for SBR and NBR-filled vulcanizing were decreased due to oxidative degradation. Additionally, the NBR-filled compounds extended more opposition to thermal degradation than SBR-filled compounds due to the high rubber-filler interaction and the presence of nitrile groups. The increase in aging temperature preferred the decrement of compressive strength at 125°C because of establishing a high oxidation process in chain scission. The aging of NR compounds filled with GRT (30 phr) was presented by *Naskar et al.*⁸⁸. It was a result that the NR vulcanizing containing GRT on aging was decreased when the particle size of GRT was decreased. Polyester cords provided the highest modulus and elasticity compared to nylon (nylon 6 and 66). It had been detected that up to 16 h of thermal aging beneath the relaxed condition, polyester recorded excellent resistance and 96% strength retention, while nylon 66 exhibited 93% strength retention. Nylon 6 exhibited inferior aging characteristics. Finally, Nylon 6 exhibited the maximum free shrinkage, changed the chain morphology, and caused poor load sharing. *Waheed et al.* evaluated the short-term aging of modified and Local Crumb Rubber (LCR) functionalized two grades of bitumen (60/70 and 80/100)⁹³. However, the increased LCR content for softer-grade bitumen results in better aging resistance. *Jovanovic et al.* tested the thermal aging (100°C for 72h and 168h) test followed out to quest the essence of aging time on the tension dimensions of rubber blend composites relying on polyisoprene (NR), polybutadiene (BR), and styrene butadiene rubber (SBR) (NR/BR/SBR=25:25:50) filled with carbon black (CB)⁹⁵.

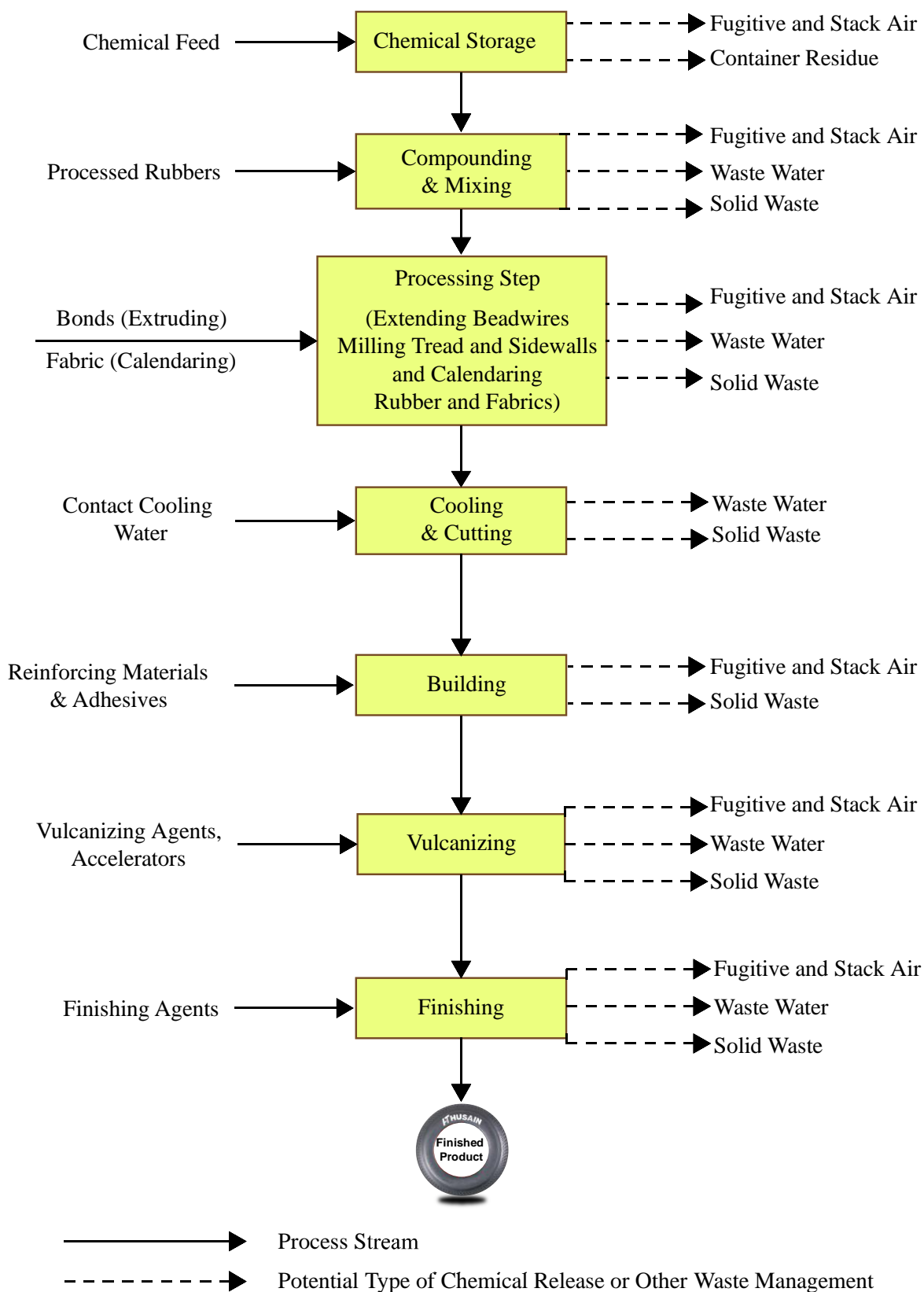


Fig. 6. The tire manufacturing process relies on mechanical properties.

Table 1. The tested visible mechanical outputs for tire composites.

Location	Composites	Hardness (°Shore)	Modulus (MPa or, kg/cm ²)	Tensile strength (kg/cm ² or N/mm ²)	Elongation at break (%)	Reference
Indonesia	SBR/NR/DRF	50-55	3	-	-	<i>Susanto et al.</i> [32]
Malaysia	WR/CF/PP	21.04	-	2.15	-	<i>Dan et al.</i> [34]
India	ELCH/DPG/SSBR	73.9	4.29	20.15	305	<i>Debnath et al.</i> [36]
Pakistan	MS/NR	36	-	11.65	958	<i>Ahmed et al.</i> [39]
India	VB/RB	-	-	24.5	417	<i>Bandyopadhyay et al.</i> [41]
India	HNBR/PA12/TPV	-	16.9	19.1-13.5	197	<i>Ismail</i> [45]
Canada	HDPE/PE-g-MA/GTR	98	468-652	-	129	<i>Fazli et al.</i> [46]
Brazil	EPDM-r	79	-	-	280	<i>Zanchet et al.</i> [49]
India	EPDM/rCB	68	9	9.6-5.9	390	<i>Sagar et al.</i> [50]
Finland	CB/MWCNT	-	2.56±0.12	16.4±60.5	467±616	<i>Poikelispaa et al.</i> [51]
China	WTR/APAO	-	>6000	-	-	<i>Yan et al.</i> [53]
Malaysia	CR	-	>1200	-	-	<i>Ali et al.</i> [56]
Malaysia	CR	-	2314	-	-	<i>Hassan et al.</i> [57]
Malaysia	CR	-	3000-3500	-	-	<i>Ali et al.</i> [58]
Poland	GTR	-	4.7	3.2-8.4	801	<i>Zedler et al.</i> [63]
India	TR/VR	-	-	145.5	400	<i>Singh et al.</i> [65]
Sri Lanka	DTBPIB/HVA-2	-	-	18	210	<i>Egodage et al.</i> [70]
Nigeria	CB/CRSS	-	-	16.8	985	<i>Akinlabi et al.</i> [83]
China	GTR-EPDM	-	-	0.72	748.2	<i>Zhang et al.</i> [86]
Serbia	NR/BR/SBR/CB	-	-	17	340	<i>Jovanovic et al.</i> [95]

The six different rubber composition results for the NR/BR/SBR blend with 0, 20, 40, 60, 80, and 100 phr of CB revealed that the tensile strength and elongation at the break of the compounds were decreased with the increased aging time in railway vehicles. It was also observed that the hardness values increased with aging. *Motiee et al.* ascertained the exploration of two-phase accountability DTG curves of the tire tread formulation based on BR-SBR ⁹⁶. It was concluded that the defined correlation is a well-acceptable method for predicting the aging period of rubber composites. The above suggestion was delivered based on BR/SBR using thermal indexes obtained from the thermal analysis curve. The aging period was efficient in the performance of BR/SBR (35/65) due to the comfortable relation between the aging times and thermal indicators attained from the thermal nature of the aged samples. *Rahmah et al.* attributed mangosteen powder (MPP) as a good potential additive in ameliorating the aging nature of NR plump

(NRCL) combined with EPDM rubber ⁹⁷. The marked rubber aging props were requisite with a higher quantity of MPP because of the natural AO, which was MPP having high-rich polyphenols that behaved as UV interceptors, causing potential resistance to oxidation. *Ibrahim et al.* monitored the binder aging in bitumen, which improved the viscosity, softening point, loss modulus, and storage modulus. Afterward, they developed the rutting resistance, resilience, and fatigue cracking resistance of asphaltic mixes ⁹⁸. The aging chemical mechanism of CRMB was imported to be looked at, leading CRMB to have a feasible viscosity to be implemented in the action. Moreover, the chemical justification of CRMB has enhanced the CRMB nature of crumb rubber-modified bitumen under aging. Natural rubber and synthetic elastomers deteriorated due to the contribution to aging observed by *Shelton* ⁹⁹. The potential factors such as heat, light, oxygen, and ozone were demanded upon the oxidation reaction of the vulcanized elastomers produced by

thermal oxidation. The authors have sought to exemplify the present state of the statement on aging and oxidation of elastomers established in the situation. The air aging test results of the specimens were found to be excellent in a ratio of blends that could potentially be applied in automotive. *Alawais et al.* examined the mechanical features of rCB with N550 carbon black before and after aging. Heat aging showed potential in the mechanical features, which was detected¹⁰⁰. *Moon et al.* justified the natural rubber/butadiene rubber (NR/BR) blends for the tire manufacturing process, relying on mechanical properties (Fig. 6), providing the kinship between the strain energy density and the crosslink density under the aging behavior of NR/BR blends. It was confirmed that the crosslink density of the aged specimen increased by about 33.9% at room temperature¹⁰¹⁻¹⁰³. Moreover, *Wang et al.* justified that HTPB-IPDI-TPH proposed the best thermal stability with thermo-oxidative aging to NR vulcanizing than TPH. Latterly, FTIR-ATR analysis exhibited that the carbonyl group in NR vulcanizing-controlling HTPB-IPDI-TPH was lower than that of TPH after thermo-oxidative aging because of the hydrogen-donating ability of the amino groups (NHCOO groups) in HTPB-IPDI-TPH during thermo-oxidative aging, which could rectify the phenolic structures of thermo-oxidative aging resistance^{104, 105}. There are some mechanical features of several chemical composites, which are critical tests for tire technology research areas mentioned in Table 1.

3. Examining rubber using DSC and TGA alongside assessing microstructural changes associated with aging

Thermogravimetric analysis (TGA) and differential scanning calorimetry (DSC) are practical methods for analyzing rubber's aging and thermal characteristics. This summarizes the steps and techniques used to evaluate aging-related microstructural alterations. The heat flow connected to rubber transitions is measured by DSC. Glass transition temperature (T_g) can change with age due to oxidation, crosslinking, or plasticizer loss. Semi-crystalline rubber can show changes in crystallinity due to degradation or prolonged stress. Oxidative stability variations in heat flow during oxidative breakdown can indicate aging effects. TGA measures the weight loss as the rubber is heated, offering information into thermal stability, as breakdown temperatures and weight loss rates may alter with aging.

The TGA/DSC analyzer was used to examine the freeze-dried extracts' thermal stability by *Mastowski et al.* The analysis was conducted in a nitrogen flow at 60 mL/min between 25 and 600 °C with a heating rate of 10 °C/min. The thermogravimetric analysis examined freeze-dried extracts' thermal stability to acquire TG and DTG curves from ambient temperature to 600 °C. It can be concluded from examining the graph, including the TG measurement

findings, that the maximum mass loss of all samples happened between 120 and 500 °C, leaving the overall residual at 600 °C with 35–40% of the initial weight. A significant proportion of residual mass was noted because the study was conducted in a non-oxidizing atmosphere. With multiple peaks associated with secondary metabolites like phenolic compounds, the second stage was recorded between 150 and 350 °C. This enhanced natural rubber-based vulcanizates' mechanical strength and aging resistance, making them suitable as bio-additives for elastomer mixtures¹⁰⁶. According to the thermal behavior (TGA) data, the heating rate has an impact on water-resistant oil (WRO) breakdown was investigated by *Aljarmouzi et al.* According to the DSC experiments, zero shear viscosity occurs when the contact temperature rises, improving WRO flow ability. The elastic stability of the water-temperature resistant (WTR) regenerated asphalt was improved by both short-term and long-term aging processes. The short-term asphalt treatment also enhances WTR swelling and absorption processes in the heated, revitalized rubber-oil-asphalt binder. The results of the segregation test showed that, in comparison to the asphalt rubber binder, the storage stability was improved by mixing waste oil with WTR and asphalt. On the other hand, pre-swelling and WTR function surface activation enhanced storage stability. It was better to employ WTR with Waste Cooking Oil (WCO) or Waste Engine Oil (WEO) to increase the compatibility of regenerated asphalt with WTR. However, because of its storage stability, rubber oil asphalt showed the least tendency to separate; at the same time, rubber oil and asphalt had the best compatibility¹⁰⁷. TGA was used to control the degree of deterioration to <5% and characterize the impact of the degrees of degradation on the polymer thermal properties, such as the initial decomposition temperature, maximum rate of decomposition, and percent residue left. Nylon-6, a semi-crystalline polymer, was selected and examined using known glass transition and melting temperatures that permit heat deterioration. Chain scission drastically altered the polymer's viscosity, flow characteristics, and processing quality by lowering its molecular weight and weight distribution. Thermogravimetry was used in accelerated degradation experiments to examine breaking functional materials' processes and chemical reactions at regulated temperatures and moisture levels¹⁰⁸. The T_g value reflected the limited mobility of the rubber chain caused by the good rubber–filler interaction in filled composites. It was evident that the untreated zirconia-filled composite (In-Zr-20) has a 5% immobilized rubber layer on the filler surface. Still, the bis[3-(triethoxysilyl)propyl] tetrasulfide (TESPT) and (3-Aminopropyl)triethoxysilane (APTES) treated zirconia-filled composites had immobilized rubber layers that were around four times (23.19%) and seven times (37.50%), respectively. Chloroprene rubber (CR) was renowned for its age resistance property, which was supplied by the electronegative chlorine atom, which deactivated

the double bond of CR. By contrasting the mechanical characteristics of the synthesized composites before and after thermal aging at 100 °C for 72 hours, the aging resistance of the composites was investigated. Chemical interactions between the chlorine atom of CR and the silanol group on the zirconia surface could result in post-curing by creating more cross-linkages¹⁰⁹. According to the DSC thermogram, n-octacosane's melting and solidification enthalpies were 201.6 J/g and 197.8 J/g, respectively, examined by *Tyagi et al.* However, the freezing and melting temperatures were found to be 53.9 °C and 51.3 °C, respectively. Using the DSC method, the latent heat, freezing point, and melting point of microencapsulated n-octacosane were determined to be 86.4 and 88.5 J/g, 53.2 °C, and 50.6 °C, respectively. The TGA study revealed that the microencapsules exhibited exceptional chemical reliability and degraded in two stages. The TGA data showed that adding NaCl to the nanocapsules can improve their thermal stability, and they came to the conclusion that n-tetradecane phase change material (PCM) might be used to improve heat transfer in thermal energy storage applications. The DSC and TGA analysis findings showed that the total dispersion of carbon and white fillers (TDCW) had high latent heat, stability, and excellent thermal reliability. Additionally, TDCW's thermal conductivity was 114% higher than that of pure thermal degradation, which composite was suggested as a possible PCM because of its inexpensive cost and high latent heat storage capacity¹¹⁰. Four styrene-butadiene-styrene (SBS) copolymer types with varying residual SB di-block contents were chosen for this study and mixed with base asphalt to create styrene-butadiene-styrene maleic anhydride (SBSMA). Each group's aging samples were created using the pressure aging vessel (PAV) and the rolling thin film oven test (RTFOT). In the gel permeation chromatography (GPC) test, SBS's Mn and Mw and SBSMA's Mw showed a declining trend with age, but SBSMA's Mn trend was the reverse of Mw's. As the residual SB content increased, so did the degree of molecular weight reduction of SBS and SBSMA. Regarding the SBS and SBSMA FTIR tests, the CI, DT, IC=C, and DP, IC=C showed an increasing trend as the residual SB content increased. These results suggested that when SBS aged, the -C=C- link cracked and produced a C=O bond. As the amount of residual SB in SBS increased, the T0 and TDTG max values of SBSMA fell in the TG test, indicating that a high residual SB in SBS impaired the thermal stability of SBSMA. This aims to investigate how the residual SB di-block in SBS affected the thermo-oxidative aging characteristics of SBS and SBSMA. Ultimately, the DSR was used to examine the rheological characteristics of SBSMA both before and after aging, and the relationship between the aging-induced changes in SBSMA's rheological parameters and chemical structure was further investigated¹¹¹. To improve the mechanical qualities, flame resistance, and anti-ultraviolet aging performance of ethylene-

vinyl acetate (EVA)/magnesium hydroxide (MDH) composites, cerium oxide (CeO₂) was added. Extrusion and injection molding were used to create the target EVA/MDH/CeO₂ composites, and thermogravimetric analysis (TGA) and differential scanning calorimetry (DSC) were used to examine the impacts of the CeO₂ addition. When CeO₂ was added, the elongation at break and Young's modulus can often be increased by 52.25% and 6.85%, respectively, compared to EVA/MDH. The EVA/MDH/CeO₂ composite's peak heat release rate (pHRR) dropped significantly from 490.6 kW/m² to 354.4 kW/m². It was discovered that CeO₂ and MDH work very well together in the composites to preserve the mechanical qualities while providing anti-UV effects. Interestingly, CeO₂ and MDH provided a new and easy way to enhance filler-polymer interaction and dispersion, improving the composites' mechanical qualities, flame retardancy, and anti-UV aging performance¹¹². According to the findings of earlier thermogravimetric analyses, the thermal stability of wet-processed vulcanized compound (WPVC) composites declined with increased sulfur-sulfur crosslinking (SSC) reinforcement. However, adding SSC did not affect the overall thermal stability of WPVC/SSC. Conversely, adding sulfur solution oil (SSO) improved the thermal stability of composites at low temperatures (less than 300 °C). The DSC spectra of WPVC and its composites with 20 and 40 weight percent SSC are displayed using a differential scanning calorimeter. The endothermic glass transition peak of WPVC appeared to be at 63°C, which was consistent with research on plasticized PVC. As the amount of SSC filler increased, the peak shifted toward higher temperatures¹¹³. *Yang et al.* used the TGA/DSC analyzer. They indicated that both swollen solution styrene-butadiene rubber (SMNR) and pre-vulcanized SMNR specimens could simultaneously obtain their TGA and DTG results. By examining the TGA and DTG values, it was possible to determine the composition element of each SMNR specimen by validating the material decomposition temperature. According to the TGA data, palmitic acid comprised 12%±6% of the entire weight, whereas NRL constitutes roughly 80%±8% of each pre-vulcanized SMNR. Increasing the amount of palmitic acid lowered the NRL content; however, the amount varied even when the sulfur level was the same. During specimen preparation, palmitic acid physically crosslinked to the rubber molecule, readily diffusing as flashes with water. Given that the compounding process involved a larger quantity of potassium palmitate, it made sense to anticipate that more palmitic acid was coupled with rubber molecules¹¹⁴. For acrylonitrile-butadiene rubber (NBR), a novel potassium methyl silicate (PMS) was used as a nano-type antioxidant. NBR/PMS composites were created by adding different amounts of the manufactured chemical as PMS (anti-aging agents) to increase the composite's resistance to heat. Consequently, the mechanical properties of the NBR/PMS composite were greatly enhanced and

outperformed by the NBR/TMQ composites with comparable filler amounts. Additionally, adding PMS (an antioxidant) decreased the NBR composites' crosslinking density, significantly impacting the mechanical properties. The findings showed that PMS significantly improved NBR/silica composites' resistance to solvent extraction and thermo-oxidative aging more effectively than 2, 2, 4-trimethyl-1, 2-dihydroquinoline (TMQ). It is demonstrated how the sample's weight steadily drops as the temperature rises. The primary criteria employed to demonstrate the thermal stability of the synthesized polymers were TGA data about the temperatures corresponding to 15% weight loss (T15), 50% weight loss (T50), 90% weight loss (T90), and maximum weight loss (Tmax). There was good agreement between the data from the TGA thermograms and the DSC curves. TGA determines the tested sample's thermal stability and stages of thermal deterioration. The DSC thermographs showed that the produced PMS polymers exhibited thermo behavioral variability in the temperature range of 141.8 to 471 °C at five different intervals. Before the DSC peak appeared, the mass loss in curing brought on by the cleavage of PMS end groups stopped. Describing the last cleavage stage between 447.6 °C and 471 °C would be simple. SiO₂ stays in the crucible after the silica-bound methyl group in the PMS is oxidized, releasing CO₂ and H₂O. The peak in the DSC results with a maximum temperature of 471 °C was caused by this potent exothermic oxidation process. This work broadened the use of PMS to create innovative and potent antioxidants for elastomers¹¹⁵. At 303 °C, the ACH sample's TG curve exhibited a single turning point, and its ultimate mass residual ratio is 68.6%. It was implied that the n-cyclohexyl-2-benzothiazole sulfonamide (NCH) and ammonium chloride (ACH) samples are simpler to transfer into the second pyrolysis phase because their initial mass loss stages concluded at lower temperatures than those of the NH sample. The ACH sample exhibited a greater mass residual ratio than the NCH sample, which suggested more inorganic fillers. The second mass loss stage (at 290–340 °C) of the NCH sample's TG curve had no clear conclusion, possibly due to variations in the samples' constituent parts. The black spectra represented the first mass loss stage at a 95% mass residual ratio, while the last mass loss stage at a 76% mass residual ratio is represented by the red spectra¹¹⁶. Microplastic thermal characteristics were marginally altered by mechanical fragmentation. According to TG/DTG research, masterbatches of brominated materials (MP-BM) breakdown temperature was lower than the master batch of chlororubber (MP-CR), suggesting that its heat resistance decreased with age. Fragmentation drastically changed surface morphology, which impacted their physicochemical properties. The oxygen-to-carbon (O/C) ratio and color index (CI) were also used to quantify the degree of aging, and their combined analysis offered a thorough assessment. The excitation energy and kinetics of

mechanical fragmentation, powered by free radical processes, differed from those of conventional aging techniques. Furthermore, the CI and O/C ratios were important in determining the aged MPs' greater heavy metal adsorption capabilities. Although the results may alter depending on the molar mass or reinforcement used, this work offered insights into the mechanical fragmentation of MPs and a novel method for assessing their environmental interactions¹¹⁷. The weight loss rate of the material was shown by the DTG curve, which was obtained from the first-order derivative of the TG curve from *Deng et al.* Five different types of asphalt were ranked according to their decomposition rates: PE-A ≈ BA > CMA > PCB-A > SPE-A. Specific processing energy (SPE) accelerated the decomposition rate by increasing the percentage of lighter components in asphalt. On the other hand, Polychloroprene blends (PCB) absorbed lighter components, increasing the onset temperature and slowing down disintegration without changing the termination temperature. Although SPE and PCB altered components in distinct ways, they both quickened the pace of breakdown. Polyethylene (PE) barely affected the rate. Better stability at high temperatures was shown by carboxylated methylstyrene-acrylonitrile's (CM-A) somewhat lower maximum breakdown rate than butyl acrylate (BA). The ash content of the five asphalt samples was determined by measuring the residual mass at 600 °C. Except for the PCB-A and CM-A samples showing somewhat greater ash content than BA, there were no notable variations in the asphalt samples' ash contents, which ranged from 16% to 21%. The TG-DTG curve of CM-A and BA was similar in this investigation, suggesting that CM-A and BA had similar levels of thermal stability. During the compounding process, the effects of PCB and SPE on asphalt's thermal stability appeared to balance one another out. Conversely, PE had a less substantial effect on asphalt's thermal behavior. The DSC curves demonstrated that, except PE-A, all four asphalt samples showed a heat absorption peak between 40 and 50 °C. Because asphalt was a complex mixture of hydrocarbons with varying molecular weights and non-metallic derivatives, its melting point was not constant. The saturated part of asphalt was very crystalline despite the resin and aromatic fractions having minimal crystalline substance¹¹⁸. The impact of the thermo-oxidative stabilizer's particle size on how well it improved the thermo-oxidative stability of poly(methyl vinyl) methylsiloxane (PVMQ) was investigated. After assessing the impact of thermo-oxidative stabilizer particle size on the mechanical performance of aged PVMQ, PVMQ composites containing additional stabilizers were added. After three hours of age, it was evident that all samples' mechanical performance dramatically declined. CeSnO-8 raised the average thermal breakdown activation energy of PVMQ composites from 94.3 KJ/mol of blank PVMQ to 112.0 KJ/mol, and T1% of TG increased by 42.7 and 31.2 °C in comparison to the blank PVMQ sample. The effect of CeSnO-x

composite oxides on the thermo-oxidative stability of PVMQ is characterized using TGA¹¹⁹. The impact of nanofiller dispersions on EPDM-based nanocomposites, including carbon-based materials (CB, nonfunctionalized and functionalized carbon nanotubes (fCNT), graphene, etc.) and inorganic-based particles (nanosilica, nanoclay, tungsten bronze nanorods, tungsten oxide, etc.), had been assessed in several studies using TGA/DTGA analysis. The nanofiller's surface chemistry may jeopardize the compatibility between the filler and the polymeric matrix, namely the presence or lack of active functional groups. The interactions between the fillers and the polymer matrix can be physical or chemical, and they depend on the development of aggregates caused by these interactions. The particle's morphology should also be considered because its dispersion and interaction with the polymeric matrix might be impacted by its specific surface area, which should be hundreds of square meters per gram. To work together, the right polymeric matrix must be chosen for nanofillers and polymeric matrices. Compared to conventional rubber matrices, EPDM-based nanocomposites have several benefits, such as the capacity to absorb significant quantities of nanofillers, which can significantly improve their characteristics and broaden their range of applications¹²⁰.

A thorough thermal profile can be obtained by combining DSC and TGA. Tensile strength, elongation at break, and hardness are assessed before and after aging by correlation with mechanical testing. Further details on damping behavior and viscoelastic characteristics can be found using dynamic mechanical analysis (DMA).

4. Discussions on the glass transition point, as this property significantly impact on the material characteristics of rubber

A key component of rubber technology, the glass transition point, directly impacts rubber's mechanical and functional properties. The glass transition temperature (T_g) is a range where the molecular mobility of the polymer is significantly reduced, as opposed to an abrupt phase transition like melting. Rubber is stiff and unyielding below T_g , making it unfit for standard uses. It acquires the suppleness and flexibility necessary for functional usage above T_g . Several elements, including chemical composition, fillers, plasticizers, crosslinking, and polymer structure, influence rubber's T_g . However, while designing and formulating rubber compounds, it is essential to comprehend and manage T_g .

Tian et al. used the atomic force microscopy-quantitative nanomechanical mapping (AFM-QNM) technique to quantify the thickness and nanomechanical performance of the interface of silicon dioxide with solution styrene-butadiene rubber (SiO_2 /SSBR) composites. The results of the AFM-QNM technique were confirmed by fitting the force

deformation curves using the Johnson-Kendall-Roberts (JKR) contact model. The dynamics of the chain segments and the formation mechanism of the interfacial structure in SiO_2 /SSBR composites with varying degrees of CA graft on SiO_2 revealed, and a new understanding of the impact of filler/polymer matrix interaction on their chain segment dynamics and glass transition temperature (T_g) proposed. The interfacial thickness of the LBR layer increased significantly with the degree of graft of CA on SiO_2 , and the dispersion of SiO_2 in the matrix became more homogeneous. This study helped better understand interfacial interaction and guided the design of interfaces to achieve high-performance polymer nanocomposites for their wider application in industry. Consequently, the interfacial SSBR layer's overall area significantly expanded, resulting in a notable drop in the SSBR matrix's chain density and increased free volume. At a higher degree of graft, a significant reduction in T_g and an enhancement in $\tan \delta_{\max}$ thus achieved¹²¹. This study examined the hydrogenated nitrile butadiene rubber (HNBR) system's glass transition temperature (T_g) and the N_2 gas pressure. The impacts of loading, filler types, acrylonitrile (ACN) content, and cross-linking density in HNBR were investigated, along with their relationship to the pressure dependency of T_g . The glass transition temperature decreased as pressure increased in the unfilled and uncross-linked HNBR system with 36% ACN, and N_2 's solubility in the elastomer also increased. The ACN content significantly influenced the pressure dependency of T_g in the HNBR system. The findings will significantly aid in comprehending the mechanism of T_g in a high-pressure gas environment and offer additional information regarding T_g 's pressure dependence. Therefore, the performance of the elastomers under high-pressure settings would be enhanced by comprehending and measuring the behavior of T_g change in a high-pressure gas environment¹²². According to the results, the non-irradiated NBR's glass transition temperature (T_g) was -69.01°C . This indicated that the NBR76 rubber's degree of cross-linking increased as the amount of irradiation increased, which in turn caused an increase in T_g . Additionally, it demonstrated an increase in the radiation cross-linking between the rubber's molecular chains. The final elongation at break reduced, and the hardness rose, according to the macroscopic properties¹²³. The rubber/glass transition of carboxylated styrene-butadiene (CSB) rubber occurred during the storage process, involving the migration of water molecules. The appropriate addition of dextran with high molecular weights, which offers many hydrophilic sites or intermolecular space to enhance CSB's water retention and prevent the long-term retrogradation of amylopectin, is linked to the reduced hardening of CSB. Starch retrogradation typically occurred in the rubbery state of CSB at 4°C , a temperature higher than the T_g of CSB, as indicated by the T_g values of freeze-dried CSB powders under various RH storage conditions. It

was crucial to slow water loss or limit water adsorption to retard the formation of the double helical structure of starch granules during the rubber/glass transition of CSB. Dextran with high molecular weights can offer numerous hydrophilic sites and intermolecular space to bind water molecules and thus reinforce the interactions between denatured gluten and gelatinized starch in CSB, inhibiting starch retrogradation. Meanwhile, the hydroxyl groups in dextran could adsorb water molecules from the storage environment of CSB above T_g. Hence, storing amorphous CSB powders below their glass transition temperature (T_g) is recommended to prevent amylopectin retrogradation and maintain stable quality¹²⁴. It was evident from Alamfard et al. that glass transition temperatures were determined by calculating the density for a range of temperatures from 40 K to 500 K with a 20 K step and a constant pressure of 1 atm. The sulfur chains' molar mass and length increase the crosslinked polybutadiene's glass transition temperature (P_B). When the crosslinked structure is made of mono-sulfur (S₁), the glass transition temperature is 179.73 K; however, when the crosslinked structure is made of octa-sulfur (S₈), the glass transition temperature rises to 215.91 K. The crosslinked P_B's density increases with the sulfur chain's length. This is because the molar weight and compactness of the network are increased by the mass and packing efficiency of longer sulfur chains compared to shorter ones. Furthermore, a change in the thermal expansion coefficient is shown when the slope of the density–temperature curves shifts at T_g. Because the slope was steeper below the T_g, the crosslinked P_B contracts more when cooled in the glassy condition. The crosslinked P_B expanded less when heated in the rubbery state because the slope was flatter above the T_g. This occurred due to the crosslinked P_B's increased segmental mobility and free volume above T_g, which lessened thermal contraction and expansion¹²⁵. The entropic elasticity of crosslinked networks dominated the samples that exhibited temperature-dependent modulus increases. Conversely, a modulus that decreases with increasing temperature suggests that the enthalpy effect is more important. At substantial loadings, a temperature-dependent behavior in the sample was shown, which concluded that energetic factors were responsible for the modulus reduction with temperature (beyond the glass transition) for this sample¹²⁶. Furthermore, the relationship between glass transition temperature (T_g) and frequency is shown for all generated samples with varying ferric oxide and waste rubber contents. T_g decreased the material's flexibility and limited the movement of segments of polymeric molecules at relaxation temperatures as waste rubber and Fe₂O₃ concentrations were uplifted. This observation confirmed that these elements had a reinforcing effect. Additionally, the activation energy (E_a) for the relaxation process at the transition area can be determined because T_g grew with frequency, a relationship that the Arrhenius relationship can

explain. This indicated reduced polymer chain mobility and greater activation energy to move the chain. The dynamic mechanical response of polymer composites to changing temperature conditions is better understood in these findings¹²⁷.

Conclusion

The rubber chemistry sketched in tire manufacturing has been outstandingly witnessed in advance of the mechanical properties under moderate hardness, modulus, tensile strength, elongation at break, and aging activity in this study. This case portends the global form of the stress-strain relationships under a sort of stiffness, the magnitude of the extension for several chemical structures, and the effects of temperature on the extrusion of tire rubber. Besides, the feasible adjustment of DSC & TGA assessment is responsible for designing actual compound formulations of the tire. It will be potentially noteworthy that the chemical and mechanical combination based on glass transition point is the dynamic line of research that has been imparted to create automotive tire agents. However, this review will offer opportunities for investigators to explore tire technology and performance further.

Consent for publication

Not applicable.

Funding

None

Conflict of interest

The author declares no conflict of interest, financial or otherwise.

Acknowledgments

Declared none

References

1. T. R. Vijayaram, A technical review on rubber, *International Journal on Design and Manufacturing Technologies*, **2009**, 3, 25-37.
2. J. Alvarez, M. Amutio, G. Lopez, L. Santamaria, J. Bilbao, M. Olazar, Improving bio-oil properties through the fast co-pyrolysis of lignocellulosic biomass and waste tires, *Waste Management*, **2019**, 85, 385-395, DOI: <https://doi.org/10.1016/j.wasman.2019.01.003>.
3. N. Antoniou, A. Zabaniotou, Features of an efficient and environmentally attractive used tires pyrolysis with energy and material recovery, *Renewable and Sustainable Energy Reviews*, **2013**, 20, 539-558, DOI: <http://dx.doi.org/10.1016/j.rser.2012.12.005>.
4. D. D. Arhin, S. A. Mensah, A. Yaya, B. A. Tuffour, Application of discarded rubber car tires as synthetic coarse aggregates in light weight pavement concretes, *American Journal of*

- Materials Science, **2015**, 5, 75-83, DOI: 10.5923/j.materials.20150504.01.
5. A. H. Ali, Influence of crumb rubber modifier on performance characteristics of stone mastic asphalt, Master thesis, Faculty of engineering, University of Malaya, **2013**.
 6. S. Bandyopadhyay, S. Dasgupta, N. Mandal, S. L. Agrawal, S. K. Mandot, R. Mukhopadhyay, A. S. Deuri and S. C. Ameta, Use of recycled tire material in natural rubber based tire tread cap compound: part i (with ground crumb rubber), Progress in Rubber, Plastics and Recycling Technology, **2005**, 21, 299-317.
 7. S. Bandyopadhyay, S. L. Agrawal, R. Ameta, S. Dasgupta, R. Mukhopadhyay, A. S. Deuri and S. C. Ameta, Recycling of waste RFL (Resorcinol-Formaldehyde Latex) dip solid in natural rubber-based ply skim compound, Progress in Rubber, Plastics and Recycling Technology, **2007**, 23, 181-193.
 8. J. M. Bouvier and M. Gelus, Pyrolysis of rubber wastes in heavy oils and use of the products, Resources and conservation, **1986**, 12, 77-93.
 9. P. Sajith, M. T. Ummer, N. Mandal, S. K. Mandot, S. L. Agrawal, S. Bandyopadhyay, R. Mukhopadhyay, B. D. Cruz, A. S. Deuri & A. P. Kuriakose, Synthesis of cobalt complexes and their evaluation as an adhesion promoter in a rubber-steel wire system, Journal of Adhesion Science and Technology, **2005**, 19, 1475-1491, DOI: 10.1163/156856105774805868.
 10. C. Sangiorgi, P. Tataranni, A. Simone, V. Vignali, C. Lantieri, G. Dondi, Stone mastic asphalt (SMA) with crumb rubber according to a new dry-hybrid technology: A laboratory and trial field evaluation, Construction and Building Materials, **2018**, 182, 200-209, DOI: <https://doi.org/10.1016/j.conbuildmat.2018.06.128>.
 11. A. A. Abdulnabi, Effects of particle size and weight percentage of waste rubber crumbs on the performance of compounded tires, Thesis: Doctor of Philosophy, School of Graduate Studies, University Putra Malaysia, **2018**.
 12. Mullins, Effect of stretching on the properties of rubber, Journal of Rubber Research, **1947**, 16, 275-289.
 13. C. Radheshkumar and J. Karger-Kocsis, Thermoplastic dynamic vulcanisates containing LDPE, rubber, and thermochemically reclaimed ground tire rubber, Plastics, Rubber and Composites, **2002**, 31, 99-105, DOI: <http://dx.doi.org/10.1179/146580102225003074>.
 14. A. K. C. Aziz, T. Z. Zaeimoedin, M. M. Kamal, Effect of vulcanization additive on cure characteristics and physical properties of silica filled epoxidised natural rubber truck tire tread compound, Advanced Materials Research, **2015**, 1107, 113-118, DOI: 10.4028/www.scientific.net/AMR.1107.113.
 15. M. Sienkiewicz, H. Janik, K. B. Labuda, J. K. Lipka, Environmentally friendly polymer-rubber composites obtained from waste tires: A review, Journal of Cleaner Production, **2017**, DOI: 10.1016/j.jclepro.2017.01.121.
 16. J. R. Learn, The effect of heat aging upon silicone rubber compounds, **1949**, Honors theses, DOI: <https://digitalworks.union.edu/theses/2231>.
 17. S. Wang, Y. Gao, K. Yan, L. You, Y. Jia, X. Dai, M. Chen, A. Diab, Effect of long-term aging on waste tire rubber and amorphous poly alpha
 18. olefin compound modified asphalt binder and its mixtures, Construction and Building Materials, **2020**, DOI: <https://doi.org/10.1016/j.conbuildmat.2020.121667>.
 19. C. J. Wellappili, K. Silva, M. Dharmatilake and I. Denawaka, Effect of Chemically Treated Buffing Dust on Technological Properties of Tire Tread Compounds, Progress in Rubber, Plastics and Recycling Technology, **2007**, 23.
 20. X. Wu, S. Wang, R. Dong, Lightly pyrolyzed tire rubber used as potential asphalt alternative, Construction and Building Materials, **2016**, 112, 623-628, DOI: <http://dx.doi.org/10.1016/j.conbuildmat.2016.02.208>.
 21. J. G. Sommer, Engineered Rubber Products, **2009**, pp. 14-24.
 22. A. Choudhury, A. K. Bhowmick, M. Soddemann, Effect of organo-modified clay on accelerated aging resistance of hydrogenated nitrile rubber nanocomposites and their life time prediction, Polymer Degradation and Stability, **2010**, 95, 2555-2562, DOI: 10.1016/j.polymdegradstab.2010.07.032.
 23. S. G. Kaang, C. K. Hong, D. S. Jung, C. S. Ryu, D. H. Lee, Preparation of novel fillers, named networked silicas, and their effects of reinforcement on rubber compounds, Polym Inter, **2008**, 57, 1101-1109.
 24. M. Baldwin, D. R. Bauer, K. R. Ellwood, Accelerated aging of tires, part II, Rubb Chem Technol, **2005**, 78, 336-354.
 25. A. Ahagon, M. Kida, H. Kaidou, Aging of tire parts during service. I. Types of aging in heavy-duty tires, Rubb Chem Technol, **1990**, 63, 683-697.
 26. J. H. Jung, A study on life time prediction and aging property of rubber products for automobile, M.S. thesis, Gyeongsang national Univ., **2005**.
 27. H. Wang, Z. You, B.P. Mills, Laboratory evaluation on high temperature viscosity and low temperature stiffness of asphalt binder with high percent scrap tire rubber, Constr. Build. Mater., **2012**, 26, 583-590.
 28. A. M. Fernández, C. Barriocana, R. Alvarez, Pyrolysis of a waste from the grinding of scrap tires, J. Hazard. Mater., **2012**, 203, 236-243.
 29. B. Acevedo, A. M. Fernández, C. Barriocanal, Identification of polymers in waste tire reinforcing fibre by thermal analysis and

- pyrolysis, *J. Anal. Appl. Pyrol.*, **2015**, 111, 224-232.
30. ASTM D412-16, Standard test methods for vulcanized rubber and thermoplastic elastomers-tension. ASTM International, West Conshohocken, PA, **2016**.
31. ASTM D2084-11, Standard test method for rubber property-vulcanization using oscillating disk cure meter, ASTM International, West Conshohocken, PA, **2016**.
32. ASTM D2240-15, Standard test method for rubber property-durometer hardness, ASTM International, West Conshohocken, PA, **2015**.
33. T. Susanto, R. Affandy, G. Katon, Rahmani, Thermal aging properties of natural rubber-styrene butadiene rubber composites filled with modified starch from *Dioscorea Hispida* Denst extract prepared by latex compounding method, *AIP Conference Proceeding*, **2018**, DOI: <https://doi.org/10.1063/1.5082421>.
34. M. Muller, P. Valasek, A. Rudawska and R. Choteborsky, Effect of active rubber powder on structural two-component epoxy resin and its mechanical properties, *Journal of Adhesion Science and Technology*, **2018**, DOI: 10.1080/01694243.2018.1428040.
35. M. M. P. Dan, L. A. Yu, Design and analysis a new materials of gasket pipping using waste rubber tires and coconut coir fibre, *Journal of Advanced Manufacturing Technology*, **2012**, 6, 11-27.
36. M. Muller, P. Novak, Researches of liquid contaminants influence on change of hardness of agricultural tire tread, *Research in Agricultural Engineering*, **2015**, 61, 14-20, DOI: 10.17221/66/2013-RAE.
37. S. C. Debnath, A. Das, D. Basu and G. H. Dresden, Naturally occurring amino acids: a suitable substitute of n-n/-di-phenyl guanidine (dpg) in silica tire formulation?, *Raw Materials and Applications*, **2013**, 25-31.
38. H. K. Lee, D. S. Kim, J. S. Won, D. Y. Jin, H. J. Lee, and S. G. Lee, Effects of thermal and humidity aging on the interfacial adhesion of polyketone fiber reinforced natural rubber composites, *Advances in Materials Science and Engineering*, **2016**, DOI: <http://dx.doi.org/10.1155/2016/4159072>.
39. K. R. S. Wright and P. S. Els, The effects of age on the stiffness properties of a suv tire, *Proceedings of the 19th International & 14th European-African Regional Conference of the ISTVS, Budapest*, **2017**, 25-27.
40. K. Ahmed, S. S. Nizami, N. Z. Raza and K. Mahmood, Mechanical, swelling, and thermal aging properties of marble sludge-natural rubber composites, *International Journal of Industrial Chemistry*, **2012**, 3, DOI: 10.1186/2228-5547-3-21.
41. R. He, S. Wu, X. Wang, Z. Wang, and H. Chen, Temperature sensitivity characteristics of sbs/crp-modified bitumen after different aging processes, *Materials*, **2018**, 11, DOI: 10.3390/ma11112136.
42. S. Bandyopadhyay, N. Mandal, S. L. Agrawal, S. Dasgupta, R. Mukhopadhyay, A. S. Deuri and S. C. Ameta, Effect of regenerated carbon-black on a bias tire tread cap compound, *Progress in Rubber, Plastics and Recycling Technology*, **2006**, 22, 195-210.
43. E. Buhlmann, S. Schulze, and T. Ziegler, Ageing of the new CPX reference tires during a measurement season, *Inter Noise*, **2013**.
44. N. Delchev, P. Malinova, Effect of the modified solid product from waste tires pyrolysis on the properties of styrene-butadiene rubber based composites, *Journal of Chemical Technology and Metallurgy*, **2014**, 49, 525-632.
45. S. S. Choi, J. C. Kim, Lifetime prediction and thermal aging behaviors of SBR and NBR composites using crosslink density changes, *Journal of Industrial and Engineering Chemistry*, **2012**, 18, 1166-1170, DOI:10.1016/j.jiec.2012.01.011.
46. M. A. Ismail, Modified lignin as replacement of carbon black in elastomers- For the development of sustainable tire technology, Master thesis, Department of Engineering and Chemical Science, **2020**.
47. A. Fazli and D. Rodrigue, Waste rubber recycling: a review on the evolution and properties of thermoplastic elastomers, *Materials*, **2020**, 13, DOI: 10.3390/ma13030782.
48. K. Pal, R. Rajasekar, D. J. Kang, Z. X. Zhang, S. K. Pal, C. K. Das, J. K. Kim, Effect of fillers on natural rubber/high styrene rubber blends with nano silica: Morphology and wear, *Materials and Design*, **2010**, 31, 677-686, DOI: 10.1016/j.matdes.2009.08.014.
49. S. Ramarad, M. Khalid, C. T. Ratnam, A. L. Chuah, W. Rashmi, Waste tire rubber in polymer blends: A review on the evolution, properties and future, *Progress in Materials Science*, **2015**, 72, 100-140, DOI: <http://dx.doi.org/10.1016/j.pmatsci.2015.02.004>.
50. A. Zanchet, A. Masiero, F. D. B. Sousa, and R. N. Brandalise, The influence of UV-accelerated aging process on industrial waste containing EPDM, *Recycling*, **2019**, 4, DOI: 10.3390/recycling4020025.
51. M. Sagar, K. Nibedita, N. Manohar, K. R. Kumar, S. Suchismita, A. Pradnyesh, A. B. Reddy, E. R. Sadiku, U. N. Gupta, P. Lachit, J. Jayaramudu, A potential utilization of end-of-life tires as recycled carbon black in EPDM rubber, *Waste Management*, **2018**, 74, 110-122, DOI: <https://doi.org/10.1016/j.wasman.2018.01.003>.
52. M. Poikelispaa, A. Das, W. Dierkes, J. Vuorinen, The Effect of Partial Replacement of Carbon Black by Carbon Nanotubes on the Properties of Natural Rubber/Butadiene Rubber Compound, *Journal of Applied Polymer Science*, **2013**, DOI: 10.1002/APP.39543.

53. J. Boruta, M. Behal, The effect of degradation degree of the dispersed phase on the ozone aging of rubbers filled with crushed rubber powder, *Die Angewandte Makromolekulare Chemie*, **1990**, 173-183.
54. K. Yan, S. Wang, D. Ge, J. Chen, S. T. and H. Sun, Laboratory performance of asphalt mixture with waste tire rubber and APAO modified asphalt binder, *International Journal of Pavement Engineering*, **2020**, DOI: 10.1080/10298436.2020.1730837.
55. H. V. C. Paulo, R. P. Linilson, L. A. C. Argemiro, R. A. Angela, F. Leonardo, Rubber compound aging characterization applied to finite element tire models, *Anais do Congresso Brasileiro de Polimeros*, 210-213.
56. M. A. Motar, Inner tube of al-diwanvia tire based on natural rubber blends, *Ibn Al-Haitham Journal for Pure & Applied Science*, **2010**, 23.
57. A. H. Ali, N. S. Mashaan, M. R. Karim, Investigation on aging resistance of rubberized bitumen binder, *International Journal of Environment and Bioenergy*, **2012**, 2, 33-41.
58. N. A. Hassan, G. D. Airey, R. P. Jaya, N. Mashros, M. A. Aziz, A review of crumb rubber modification in dry mixed rubberized asphalt mixtures, *Jurnal Teknologi (Sciences & Engineering)*, **2014**, 70, 127-134.
59. A. H. Ali, N. S. Mashaan and M. R. Karim, Improving asphalt resistance to aging by using waste tire rubber, *1st International Conference on Innovation and Technology for Sustainable Built Environment (ICITSBE)*, **2012**, 512-515.
60. N. S. Mashaan, A. H. Ali, M. R. Karim, and M. A. Aziz, A review on using crumb rubber in reinforcement of asphalt pavement, *The Scientific World Journal*, **2014**, DOI: <http://dx.doi.org/10.1155/2014/214612>.
61. C. N. A. Jaafar, I. Zainol, N. S. Ishak, R. A. Ilyas, S. M. Sapuan, Effects of the liquid natural rubber (LNR) on mechanical properties and microstructure of epoxy/silica/kenaf hybrid composite for potential automotive applications, *Journal of Materials Research and Technology*, **2021**, 12, 1026-1038.
62. A. Mohajerani, L. Burnett, J. V. Smith, S. Markovski, G. Rodwell, M. T. Rahman, H. Kurmus, M. Mirzababaei, A. Arulrajah, S. Horpibulsuk, F. Maghool, Recycling waste rubber tires in construction materials and associated environmental considerations: A review, *Resources, Conservation and Recycling*, **2020**, 155, DOI: <https://doi.org/10.1016/j.resconrec.2020.104679>.
63. N. A. Hassan, A. A. A. Almusawi, M. Z. H. Mahmud, N. A. M. Abdullah, N. A. M. Shukry, N. Mashros, R. P. Jaya, N. I. M. Yusoff, Engineering properties of crumb rubber modified densegraded asphalt mixtures using dry process, *IOP Conf. Series: Earth and Environmental Science*, **2019**, DOI: 10.1088/1755-1315/220/1/01200.
64. L. Zedler, M. Klein, M. R. Saeb, X. Colom, J. Canavate and K. Formela, Synergistic effects of bitumen plasticization and microwave treatment on short-term devulcanization of ground tire rubber, *Polymers*, **2018**, 10, DOI: 10.3390/polym10111265.
65. C. Loderer, M. N. Part, L. D. Poulikakos, Effect of crumb rubber production technology on performance of modified bitumen, *Construction and Building Materials*, **2018**, 191, 1159-1171, DOI: <https://doi.org/10.1016/j.conbuildmat.2018.10.046>.
66. G. Singh, A. Mahajan, M. Kumar, Comparative study of tire rubber and V-belt rubber: composition and mechanical properties, *IOSR Journal of Mechanical and Civil Engineering*, **2015**, 12, 60-65, DOI: 10.9790/1684-12516065.
67. T. Kirushanthi, D. R. Ratnaweera and U. N. Etampawalav, Crumb rubber and silica reinforced rubber composites for outdoor flooring applications, *Third Biennial International Symposium on Polymer Science and Technology*, **2017**.
68. D. Habibah, S. Saiwari, W. Dierkes, J. W. M. Noordermeer, Effect of ground tire rubber devulcanisates on the properties of a passenger car tire tread formulation, *Advanced Materials Research*, **2014**, 844, 425-428, DOI: 10.4028/www.scientific.net/AMR.844.425.
69. Y. Liu, Y. Zhang, Z. Zhang, A. M. Wemyss, C. Wan, P. Song, and S. Wang, Effective thermal-oxidative reclamation of waste tire rubbers for producing high-performance rubber composites, *ACS Sustainable Chemistry and Engineering*, **2020**, DOI: 10.1021/acssuschemeng.0c02292.
70. K. A. Owaid, Effect of aging on the rheological properties of the modified asphalt-rubber system using microwave technique, *European Chemistry Bulletin*, **2014**, 3, 668-671, DOI: 10.17628/ECB.2014.3.668.
71. S. M. Egodage, J. F. Harper and S. Walpalage, Effect of maleimide curing on mechanical properties of ground tire rubber/waste polypropylene blends, *Plastics, Rubber and Composites*, **2012**, 41, 332-340, DOI: 10.1179/1743289811Y.0000000042.
72. D. Habibah, S. Saiwari, W. Dierkes, J. W. M. Noordermeer, Influence of ground tire rubber devulcanisates on morphology and properties of tread tire formulation, *Advanced Materials Research*, **2014**, 1024, 159-162, DOI: 10.4028/www.scientific.net/AMR.1024.159.
73. S. N. Russell, R. Maharaj and A. S. George, End-of-life management of scrap tires using crumb rubber modified TLA, *International Journal of Applied Environmental Sciences*, **2011**, 6, 87-98.
74. J. L. F. Dias, L. G. P. Santos, S. D. Capita, Mechanical performance of dry process fine crumb rubber asphalt mixtures placed on the Portuguese road network, *Construction and Building Materials*, **2014**, 73, 247-254, DOI:

- <http://dx.doi.org/10.1016/j.conbuildmat.2014.09.110>.
75. D. Feldman, Natural rubber nanocomposites, *Journal of Macromolecular Science, Part A: Pure and Applied Chemistry*, **2017**, DOI: 10.1080/10601325.2017.1316671.
76. Z. Feng, W. Rao, C. Chen, B. Tian, X. Li, P. Li, Q. Guo, Performance evaluation of bitumen modified with pyrolysis carbon black made from waste tires, *Construction and Building Materials*, **2016**, 111, 495-501, DOI: <http://dx.doi.org/10.1016/j.conbuildmat.2016.02.143>.
77. K. Formela, A. Hejna, L. Zedler, X. Colom, J. Canavate, Microwave treatment in waste rubber recycling-recent advances and limitations, *Express Polymer Letters*, **2019**, 13, 565-588, DOI: <https://doi.org/10.3144/expresspolymlett.2019.48>
78. J. Fu, L. Chen, H. Yang, Q. Zhong, L. Shi, W. Deng, X. Dong, Y. Chen, G. Zhao, Mechanical Properties, Chemical and Aging Resistance of Natural Rubber Filled with Nano-Al₂O₃, *Polymer Composites*, **2012**, 404-411, DOI: 10.1002/pc.22162.
79. W. A. Halim, R. Junid, N. Sazali, Enhancement of flexural modulus and strength of epoxy nanocomposites with the inclusion of functionalized GNPs using Tween 80. *J. Eng. Appl. Sci.*, **2024**, 71, DOI: <https://doi.org/10.1186/s44147-024-00405-x>.
80. L. R. Honorato, R. C. R. Nunes, J. G. L. Cosme, L. L. Y. Visconte, A. C. C. Peres and J M. Costa, Effect of the cure system on aging resistance of natural rubber Compounds, *Journal of Elastomers & Plastics*, **2019**, 1-13, DOI: 10.1177/0095244319859604.
81. A. M. Othman, Fracture resistance of rubber-modified asphaltic mixtures exposed to high-temperature cyclic aging, *Journal of Elastomers And Plastics*, **2006**, 38, 19-30, DOI: 10.1177/0095244306059852.
82. S. M. R. S. Ismail, T. Chatterjee and K. Naskar, Superior heat-resistant and oil-resistant blends based on dynamically vulcanized hydrogenated acrylonitrile butadiene rubber and polyamide 12, *Polymer Advanced Technologies*, **2016**, DOI: 10.1002/pat.3966.
83. L. Leng, Q. Han and Y. Wu, The aging properties and phase morphology of silica filled silicone rubber/butadiene rubber composites, *RSC Advances*, **2020**, 10, 20272-20278, DOI: 10.1002/pat.3966.
84. A. K. Akinlabi, U. N. Okwu, F. E. Okieimen & N. A. Oladoja, Thermal aging properties and molecular transport of solvents through vulcanizates prepared from thioglycolic acid modified epoxidized low molecular weight natural rubber blends filled with admixtures of carbon black and carbonized rubber seed shell, *International Journal of Polymeric Materials and Polymeric Biomaterials*, **2006**, 55, 1095-1114, DOI: <http://dx.doi.org/10.1080/00914030600692091>.
85. B. Li, J. Zhou, Z. Zhang, X. Yang and Y. Wu, Effect of short-term aging on asphalt modified using microwave activation crumb rubber, *Materials*, **2019**, 12, DOI: 10.3390/ma12071039.
86. T. Zhou, J Zhou, Q Li, and B Li, Aging properties and mechanism of microwave-activated crumb rubber modified asphalt binder, *Frontiers Materials*, **2020**, DOI: 10.3389/fmats.2020.603938.
87. Y. Zhang, H. Wei and Y. Dai, Influence of Different Aging Environments on Rheological Behavior and Structural Properties of Rubber Asphalt, *Materials*, **2020**, 13, DOI: 10.3390/ma13153376.
88. A. Mostafa, A. A. Kasem, M. R. Bayoumi, M. G. El-Sebaie, The influence of CB loading on thermal aging resistance of SBR and NBR rubber compounds under different aging temperature, *Materials and Design*, **2009**, 30, 791-795, DOI: 10.1016/j.matdes.2008.05.065.
89. A. K. Naskar, S. K. De, A. K. Bhowmick, P. K. Pramanik, R. Mukhopadhyay, Characterization of ground rubber tire and its effect on natural rubber compound, *Rubber Chemistry And Technology*, **2000**, 73, 902-911.
90. A. K. Naskara, A. K. Mukherjee, R. Mukhopadhyay, Studies on tire cords: degradation of polyester due to fatigue, *Polymer Degradation and Stability*, **2004**, 83, 173-180, DOI: 10.1016/S0141-3910(03)00260-X.
91. M. Nuzaimah, S. M. Sapuan, R. Nadlene and M. Jawaid, Recycling of waste rubber as fillers: A review, *IOP Conf. Series: Materials Science and Engineering*, **2018**, 368, DOI:10.1088/1757-899X/368/1/012016.
92. Z. Xiong, Z. Tang, S. He, Z. Fang, Z. Chen, F. Liu, L. Li, Analysis of mechanical properties of rubberised mortar and influence of styrene-butadiene latex on interfacial behaviour of rubber-cement matrix, *Construction and Building Materials*, **2021**.
93. M. Nuzaimah, S. M. Sapuan, R. Nadlene, M. Jawaid, Effect of surface treatment on the performance of polyester composite filled with waste glove rubber crumbs, *Waste and Biomass Valorization*, **2021**, 12, 1061-1074, DOI: <https://doi.org/10.1007/s12649-020-01008-2>.
94. M. S. Waheed, M. Elahi, Effect of short term aging on unmodified and Local Crumb Rubber (LCR), *Quest Research Journal*, **2020**, 18, 63-70.
95. N. K. Kushwaha, M. K. Jha, Value creation of natural rubber and its alternate possibilities, 68th Annual Session of Indian Institute of Chemical Engineers, **2015**.
96. S. Jovanovic, V. Jovanovic, G. Markovic, M. M. Cincovic, J. B. Simendic, The effect of aging temperature on carbon black reinforced ternary rubber blend in railway industry, XVII International Scientific-Expert Conference on Railways, **2016**, 245-248.

97. F. Motiee, T. Bigdeli, Prediction of Mechanical and Functional Features of Aged Rubber Composites Based on BR/SBR; Structure-Properties Correlation, *Materials Research*, **2020**, 22, DOI: <https://doi.org/10.1590/1980-5373-mr-2019-0226>.
98. M. Rahmah, A. R. A. Khusyairi, H. N. Khairunnisya and M. S. Nurbalqis, Oven ageing versus uv ageing properties of natural rubber cup lump /epdm rubber blend with Mangosteen Powder (MPP) as natural antioxidant., *IOP Conf. Series: Materials Science and Engineering*, **2019**, 548, DOI: [10.1088/1757-899X/548/1/012014](https://doi.org/10.1088/1757-899X/548/1/012014).
99. M. R. Ibrahim, H. Y. Katman, M. R. Karim, S. Koting, and N. S. Mashaan, A review on the effect of crumb rubber addition to the rheology of crumb rubber modified bitumen, *Advances in Materials Science and Engineering*, **2013**, DOI: <http://dx.doi.org/10.1155/2013/415246>.
100. J. R. Shelton, Aging and oxidation of elastomers." *Rubber Chemistry and Technology*, **1957**, 30, 1251-1290, DOI: <https://doi.org/10.5254/1.3542760>.
101. A. Alawais & R. P. West, Ultra-violet and chemical treatment of crumb rubber aggregate in a sustainable concrete mix, *Journal of Structural Integrity and Maintenance*, **2019**, 4, 144-152, DOI: [10.1080/24705314.2019.1594603](https://doi.org/10.1080/24705314.2019.1594603).
102. B. Moon, J. Lee, S. Park and C. Seok, Study on the aging behavior of Natural Rubber/Butadiene Rubber (NR/BR) blends using a parallel spring model, *Polymers*, **2018**, 10, DOI: [10.3390/polym10060658](https://doi.org/10.3390/polym10060658).
103. K. M. Shatanawi, S. Biro, M. Naser & S. N. Amirkhanian, Improving the rheological properties of crumb rubber modified binder using hydrogen peroxide, *Road Materials and Pavement Design*, **2013**, 14, 723-734, DOI: [10.1080/14680629.2013.812535](https://doi.org/10.1080/14680629.2013.812535).
104. R. Maharaj, A. S. George, S. N. Russell and D. S. Ackbarali, The Influence of Recycled Tire Rubber on the Rheological Properties of Trinidad Lake Asphalt and Trinidad Petroleum Bitumen, *International Journal of Applied Chemistry*, **2009**, 5, 181-191.
105. Y. Wang, X. Zeng, H. Li & J. Guo, Structural Characterization of Hydroxyl-Terminated Polybutadiene-Bound 2, 2-Thiobis(4-methyl-6-tertbutylphenol) and its thermo-oxidative aging resistance for natural rubber vulcanizates, *Journal of Macromolecular Science, Part B: Physics*, **2012**, 51, 1904-1920, DOI: [10.1080/00222348.2012.664452](https://doi.org/10.1080/00222348.2012.664452).
106. X. Zhang, D. Tian, W. Zhang, J. Zhu, and C. Lu, Morphology, foaming rheology and physical properties of ethylene-propylene diene Rubber/Ground Tire Rubber (GTR) composite foams: effect of mechanochemical devulcanisation of GTR, *Progress in Rubber, Plastics and Recycling Technology*, **2013**, 29, 81-98.
107. M. Masłowski, A. Aleksieiev, J. Miedzianowska, M. E. Szmechtyk and K. Strzelec, Antioxidant and Anti-Aging Activity of Freeze-Dried Alcohol-Water Extracts from Common Nettle (*Urtica dioica* L.) and Peppermint (*Mentha piperita* L.) in Elastomer Vulcanizates, *Polymer*, **2022**, 14, 1-23, DOI: <https://doi.org/10.3390/polym14071460>
108. A. Aljarmouzi and R. Dong, Sustainable Asphalt Rejuvenation by Using Waste Tire Rubber Mixed with Waste Oils, *Sustainability*, **2022**, 14, 1-27, DOI: <https://doi.org/10.3390/su14148246>
109. R. R. Pagar, S. R. Musale, G. Pawar, D. Kulkarni, and P. S. Giram, Comprehensive Review on the Degradation Chemistry and Toxicity Studies of Functional Materials, *ACS Biomater. Sci. Eng.*, **2022**, 8, 2161-2195, DOI: <https://doi.org/10.1021/acsbomaterials.1c01304>
110. S. C. Ambilkar, G. L. Dhakar, B. P. Kapgate, A. Das, S. Hait, R. S. Gedam, R. Kasilingam and C. Das, Enhancing the material performance of chloroprene rubber (CR) by strategic incorporation of zirconia, *Mater. Adv.*, **2022**, 3, 2434-2446, DOI: [10.1039/d1ma00793a](https://doi.org/10.1039/d1ma00793a)
111. V. V. Tyagi, K. Chopra, R. K. Sharma, A. K. Pandey, S. K. Tyagi, M. S. Ahmad, A. Sari, R. Kothari, A comprehensive review on phase change materials for heat storage applications: Development, characterization, thermal and chemical stability, *Solar Energy Materials & Solar Cells*, **2022**, DOI: <https://doi.org/10.1016/j.solmat.2021.111392>
112. Z. Li, H. Liu, W. Chen, Y. Li, Z. Zhao, Y. Yin, M. Li, Influence of residual SB di-block in SBS on the thermo-oxidative aging behaviors of SBS and SBS modified asphalt, *Materials and Structures*, **2022**, 55, DOI: <https://doi.org/10.1617/s11527-022-01882-3>
113. J. Hobson, G. Z. Yin, X. Yu, X. Zhou, S. G. Prolongo, X. Ao and D. Y. Wang, Synergistic Effect of Cerium Oxide for Improving the Fire-Retardant, Mechanical and Ultraviolet-Blocking Properties of EVA/Magnesium Hydroxide Composites, *Materials*, **2022**, 1-15, DOI: <https://doi.org/10.3390/ma15175867>
114. M. Saied, A. Reffae, S. Hamieda and S. L. Abd-El-Messieh, Eco-friendly polymer composite films based on waste polyvinyl chloride/sunflower seed cake for antimicrobial and antistatic applications, *Pigment & Resin Technology*, **2022**, DOI: [10.1108/PRT-10-2021-0126](https://doi.org/10.1108/PRT-10-2021-0126)
115. K. Y. Yang, Development and Characterisation of Thermal Responsive Shape Memory Natural Rubber, *University of Nottingham Malaysia*, **2022**, pp. 1-88
116. D. S. Mahmoud, A. E. Elsayed, A. A. Reffae and D. E. E. Nashar, Novel prepared nano potassium methyl silicate as antioxidant for nitrile rubber, *Polymers and Polymer*

- Composites, **2022**, 31, 1–18, DOI: 10.1177/0967391123115407
117. Z. Jia, C. Xu, R. Guan, X. Wang, Y. Deng, Simulation of the Chalking of Silicone Rubber Based on Tetramethylammonium-Hydroxide-Catalyzed Scission Reaction, *Polymer Degradation and Stability*, **2023**, 208, DOI: <https://doi.org/10.1016/j.polymdegradstab.2023.110251>
118. Y. Yan, Y. Yu, J. Sima, C. Geng, J. Yang, Aging behavior of microplastics accelerated by mechanical fragmentation: alteration of intrinsic and extrinsic properties, *Environmental Science and Pollution Research*, **2023**, 30, 90993–91006 DOI: <https://doi.org/10.1007/s11356-023-28736-x>
119. Q. Deng, C. Li, Y. Gan, Y. Li, A. Chen, L. Liu, S. Yi, J. Feng, Optimizing the formulation design and investigating the composite modification mechanism of pyrolysis carbon Black/Polyethylene/Synthetic plant ester composite modified asphalt, *Construction and Building Materials*, **2023**, 406, DOI: <https://doi.org/10.1016/j.conbuildmat.2023.133468>
120. C. Cong, M. Yuan, Han Wang, R, U. D. Peng, J. Ouyang, Advancing thermo-oxidative stability in silicone rubber with cerium-tin complex oxide, *Polym Adv Technol.*, **2024**, 35, 1-16, DOI: <https://doi.org/10.1002/pat.65912024>.
121. N. L. Costa, C. T. Hiranobe, H. P. Cardim, G. Dognani, J. C. Sanchez, J. A. Jaramillo Carvalho, G. B. Torres, L. L. Paim, L. F. Pinto, G. P. Cardim, F. C. Cabrera, R. J. Santos and M. J. Silva, A Review of EPDM (Ethylene Propylene Diene Monomer) Rubber-Based Nanocomposites: Properties and Progress, *Polymers*, **2024**, 16, 1-35, DOI: <https://doi.org/10.3390/polym16121720>
122. C. Tian, S. Wang, C. Miao, C. Wang, L. Xu, N. Ning, M. Tian, Quantification of interfacial structure at nanoscale and its relationship with viscoelastic glass transition of SiO₂/elastomer nanocomposites, *Polymer*, **2023**, 271, DOI: <https://doi.org/10.1016/j.polymer.2023.125798>
123. L. Cai, X. Chen, A. K. Bhowmick, and R. Krishnamoorti, Unveiling the Pressure-Induced Dynamics on the Glass Transition Temperature of Hydrogenated Nitrile Rubber, *Macromolecules*, **2024**, 57, 8576–8587, DOI: <https://doi.org/10.1021/acs.macromol.4c01409>
124. R. Luo, D. Kang, C. Huang, T. Yan, P. Li, H. Ren and Z. Zhang, Mechanical Properties, Radiation Resistance Performances, and Mechanism Insights of Nitrile Butadiene Rubber Irradiated with High-Dose Gamma Rays, *Polymers*, **2023**, 15, 1-12, DOI: <https://doi.org/10.3390/polym15183723>
125. S. Li, R. Sun, Y. Gong, J. Cui, W. Sui, T. Wu, R. Liu, M. Zhang, Effects of dextran molecular weight on starch retrogradation and technological properties of Chinese steamed bread: Based on the rubber/ glass transition, *International Journal of Biological Macromolecules*, **2024**, 270, DOI: <https://doi.org/10.1016/j.ijbiomac.2024.131887>
126. T. Alamfard, T. Lorenz and C. Breitkopf, Glass Transition Temperatures and Thermal Conductivities of Polybutadiene Crosslinked with Randomly Distributed Sulfur Chains Using Molecular Dynamic Simulation, *Polymers*, **2024**, 16, 1-22, DOI: <https://doi.org/10.3390/polym16030384>
127. D. Dhara, M. A. Rahman, E. Ruzicka, A. Karekar, D. Vlassopoulos, K. Saalwächter, B. Benicewicz, and S. K. Kumar, Mechanical Properties of Polyisoprene-Based Elastomer Composites, *Macromolecules*, **2024**, 57, 1448–1460, DOI: <https://doi.org/10.1021/acs.macromol.3c01084>
128. M. M. A. Kader, M.T. Abou-Laila, M. S. S. El-Deeb, E. O. Taha & A. S. El-Deeb, Structural, radiation shielding, thermal and dynamic mechanical analysis for waste rubber/ EPDM rubber composite loaded with Fe₂O₃ for green environment, *Scientific Reports*, **2024**, 14, DOI: <https://doi.org/10.1038/s41598-024-62308-4>